Schweizerische Eidgenossenschaft
Confédération suisse
Confederazione Svizzera
Confederaziun svizra

Eidgenössisches Departement für Umwelt, Verkehr, Energie und Kommunikation UVEK

Bundesamt für Energie BFE
Pilot-, Demonstrations- und Leuchtturmprogramm

Schlussbericht vom 27. November 2017

Future Mobility

Hydrogen production from excess electricity with use in mobility or re-conversion to electricity

© Empa 2017

Datum: 23. Oktober 2017 (Entwurf)

Ort: Villigen, Zürich, Dübendorf

Subventionsgeberin:

Schweizerische Eidgenossenschaft, handelnd durch das

Bundesamt für Energie BFE
Pilot-, Demonstrations- und Leuchtturmprogramm
CH-3003 Bern

www.bfe.admin.ch

Subventionsempfänger:

PSI	ETH	Empa
	Rämistrasse 101	Überlandstrasse 129
5232 Villigen	8092 Zürich	8600 Dübendorf
www.psi.ch	www.ethz.ch	www.empa.ch

Autoren:

PSI: Tilman Schildhauer, Julia Witte, Frédéric Vogel
Empa: Urs Cabalzar, Marco Brügger, Christian Bach
ETH: Christian Schürch

BFE-Programmleitung: Yasmine Calisesi, yasmine.calisesi@bfe.admin.ch
BFE-Projektbegleitung: Stefan Oberholzer, Stefan.oberholzer@bfe.admin.ch
BFE-Vertragsnummer: SI/501002-01

Für den Inhalt und die Schlussfolgerungen sind ausschliesslich die Autoren dieses Berichts verantwortlich.

Bundesamt für Energie BFE

Mühlestrasse 4, CH-3063 Ittigen; Postadresse: CH-3003 Bern

Tel. +41 58 462 56 11 · Fax +41 58 463 25 00 · contact@bfe.admin.ch · www.bfe.admin.ch

Zusammenfassung

Das Projekt startete am 1. Januar 2014 und wurde am 30. September 2017 abgeschlossen. Dieser Abschlussbericht beschreibt die Resultate über das gesamte Projekt. Das Projekt ist unterteilt in die Arbeitspakete Future Mobility Demonstrator an der Empa (AP1), Methanisierung am PSI (AP2) und HCNG Feldversuche an der ETHZ und der Empa (AP3).

AP1 - Future Mobility Demonstrator an der Empa

Im Rahmen des ersten Arbeitspaketes wurde eine Power-to-Gas Anlage mit lokaler H_2 Produktion realisiert, welche folgende Komponenten umfasst: 180 kW PEM Elektrolyseur, 44 MPa Kolbenverdichter, 44 MPa Druckspeichertanks, 35 MPa H_2-Zapfsäule und 35 MPa HCNG Zapfsäule. Der Wasserstoffpfad inklusive Produktion, Verdichtung und Speicherung wurde im Jahr 2015 installiert (mit Eröffnung im November 2015) und die 35 MPa H_2-Zapfsäule ist seit diesem Zeitpunkt in Betrieb.

Zudem wurde ein Matlab Modell der Power-to-Gas Anlage entwickelt, welches die Untersuchung von Aspekten betreffend Anlagenauslegung und Betriebsstrategieoptimierung hinsichtlich Stromkosten und Verfügbarkeit erneuerbarer Elektrizität erlaubt. Auf Basis von Messungen an der Demonstrationsanlage wurden well-to-tank Analysen durchgeführt, welche aufzeigen, dass 57% (Brennwert) der elektrischen Energie den Fahrzeugtank (35 MPa) erreicht. Diese Zahl steigt auf 70% (Brennwert) für industrielle Anlagen von kleinerer Grösse. Weitere Messungen betreffend Dynamik des eingesetzten Elektrolyseurs bestätigen dessen Fähigkeit rasch auf ändernde Lastvorgaben reagieren zu können. Das Nachfahren von vorgegeben Sprüngen gelingt innerhalb von 2 Sekunden bzw. sogar Sekundenbruchteilen, je nach dem auf welche Art die Laständerung induziert wird.

AP2 – Methanisierung am PSI

Im zweiten Arbeitspaket wurde die Speicherung von Stromspitzen als (Bio-)Methan auf Basis des am PSI entwickelten hydrothermalen Vergasungs- und Methanisierungsprozesses untersucht und demonstriert. Ein Ansatz beinhaltete die Produktion von H_2 durch Elektrolyse und Miteinspeisung des H_2 mit Biomasse in den hydrothermalen Vergasungsprozess. Die Machbarkeit dieses Ansatzes wurde in der Theorie mit Hilfe von Modellen und auch in der Praxis über Experimente im kleinen Massstab auf einem Teststand mit kontinuierlicher hydrothermaler Vergasung am PSI demonstriert. Die Zugabe von H- in stöchiometrischem Verhältnis erzeugte ein Methan-reiches Gas aus Glyzerin mit (86 ± 6) vol% CH-, was dem berechneten maximalen Wert von 88 vol-% beim chemischen Equilibrium entspricht. Bei der Zugabe von H2 wurden keine schädlichen Auswirkungen auf den Katalysator festgestellt. Ein zweiter Ansatz könnte einen elektrischen Prozesserhitzer für die hydrothermale Vergasung vorsehen, welcher Stromspitzen aufnehmen würde. Falls keine Stromspitzen vorhanden sind, würde der Prozesserhitzer mit Methan-reichem Gas betrieben. Zu diesem Zweck wurde ein dualer Gas/Elektrischer-Prozesserhitzer auf Basis von kommerziell erhältlichen Komponenten konzipiert. Es konnte gezeigt werden, dass beide Ansätze zur Speicherung von Stromspitzen als (Bio)Methan unter Einsatz der hydrothermalen Vergasung realisierbar sind.

Zudem konnte das Know-how in Bezug auf die CO_2 Methanisierung (Umwandlung von Biogas und reinem CO_2, z.B. von Quellen aus der Industrie) und die H_2-reiche Methanisierung von aus Vergasung stammendem Produktgas durch Modellierung und Experimente erhöht werden. Da die Pilotanlage “GanyMeth”, welche ursprünglich verwendet werden sollte, leider nicht innerhalb der Projektzeit verfügbar war, wurden die Experimente auf der Anlage “Cosyma” (TRL 5) durchgeführt.

Im Rahmen eines anderen Projektes wurde “Cosyma” an eine Biogas Anlage in Zürich angeschlossen. Nach Erreichung der Ziele dieses anderen Projektes, wurde der Betrieb der Installation fortgeführt, um Optimierungsexperimente durchzuführen. Bei diesen Experimenten wurde festgestellt, dass die Zugabe von Wasser deutlich reduziert werden konnte ohne dass sich Koks bildete. Dies verbessert die Ausbeute im Hauptreaktor und ermöglicht die Verringerung der Aufwände (CAPEX und OPEX) für den Aufbereitungsschritt im Prozess.

Parallel dazu wurde die komplette Prozesskette von Biogas-basiertem Power-to-Gas modelliert und optimiert. Dazu wurden die Haupteinheiten (Reaktoren, Membrane) durch rate-based Modelle abgebildet, während andere Prozesseinheiten mit thermodynamischen und short-cut Modellen berechnet wurden. Die detaillierte Beschreibung von vier unterschiedlichen Prozesskonzepten ermöglichte entsprechend detaillierte Kostenberechnungen. Es zeigte sich, dass durch die Spezifikationen für die Einspeisung ins Netz ein Aufbereitungsschritt – z.B. mittels H_2-Separatormembrane oder nachgeschaltetem Festbettreaktor – nötig wird. Als optimal hinsichtlich Prozessstabilität und –flexibilität erwies sich die Nutzung einer H_2 Separatormembrane, welche aufgrund des wiederverwendeten H_2 wiederum die Bedingungen für den Hauptreaktor veränderte.

WP3 - HCNG Feldversuche an ETHZ und Empa

Das dritte Arbeitspaket umfasst Untersuchungen zur Nutzung des Treibstoffgemischs HCNG für mobile und stationäre Anwendungen. HCNG enthält H_2 (Wasserstoff) und CNG (Erdgas/Biogas), wobei der Schwerpunkt auf eine H_2-Beimischung von 0 bis 25 vol% für mobile und 0 bis 50 vol% für stationäre Anwendungen gelegt wurde.

Um die Betankung von drei CNG Testfahrzeugen zu ermöglichen, wurde in einem ersten Schritt eine temporäre Betankungslösung realisiert, welche eine niedrige H_2-Beimischung von 2 vol% erlaubt. 2 vol% entsprechen dem maximal zugelassenen H_2-Anteil für konventionelle CNG Fahrzeuge. Die Testfahrzeuge wurden mehrere Monate mit reinem CNG und mit einer Beimischung von 2 vol% H_2 als Teil der Paketauslieferungs-Flotte der Schweizerischen Post betrieben. Dabei wurden Motordaten mittels onboard-Aufzeichnungsgeräten erfasst.

Die Analyse der Daten zeigten leichte Tendenzen zu verbesserter Effizienz und sinkenden CO_2-Emissionen auf, welche höchstwahrscheinlich auf den verbesserten Verbrennungsprozess zurückzuführen sind. Die Menge an beigefügtem H_2 war allerdings sehr klein, sodass der Effekt innerhalb der statistischen Unsicherheit liegt. Es konnte jedoch festgestellt werden, dass sich das Motorstartverhalten deutlich verbessert.

Im Allgemeinen konnte bestätigt werden, dass die Beimischung von geringen Mengen an H_2 zum Treibstoff für konventionelle CNG-Fahrzeuge keine negativen sondern eher positive Effekte hervorrufen, obwohl keinerlei Modifikationen an den Testfahrzeugen vorgenommen wurden. Zu dieser Thematik ist derzeit die Erstellung einer Publikation in Arbeit, welche Anfang 2018 eingereicht werden soll.

Für die Feldversuche mit höherer H_2 Beimischung (bis 25 vol%) wurde ein CNG-Lieferwagen umgerüstet, wobei neue Tanks und Treibstoffleitungen installiert wurden um die H_2-Verträglichkeit zu gewährleisten. Das neue Treibstoffsystem und das Fahrzeug als Ganzes wurden re-zertifiziert und das Fahrzeug hat den Feldversuch in der Paketauslieferungs-Flotte der Post im Sommer 2017 gestartet. Parallel dazu wurde eine permanente Lösung zur Betankung von HCNG realisiert, welche die Beimischung von 0 bis 30 vol% H_2 ermöglicht. Die Konstruktion und der Steuerungsalgorithmus dieser HCNG-Zapfsäule wurden an der Empa entwickelt und basieren auf Messungen und Simulationen, welche im Rahmen dieses Projektes ausgeführt wurden. Während der Feldversuche waren weder im CNG- noch im HCNG-Betrieb negative Effekte feststellbar und die HCNG Zapfsäule funktionierte so zuverlässig wie eine konventionelle CNG-Zapfsäule.

In Bezug auf stationäre Anwendungen wurde der Einfluss von HCNG auf eine Mikro-Kraft-Wärme-Kopplungsanlage (Mikro-KWK) untersucht. Dabei wurde der Schwerpunkt auf die Analyse der Auswirkungen von H_2-Beimischung auf den Verbrennungsprozess und die Rohemissionen bei Magerbetrieb und Abgasrückführung (AGR) gelegt. Die Messungen wurden an einem fremdgezündeten Einzylinder 4-Takt Saugmotor mit 250 cm^3 Hubraum durchgeführt. Der Teststand umfasste eine vorgelagerte Gasmischeinheit, welche vordefinierte Mengen an AGR und H_2 dem Motor zuführte.

Es zeigte sich, dass mit Hilfe der H_2-Beimischung die Betriebsgrenzen eines Mikro-KWK mit Saugmotor im Magerbetrieb von $\lambda = 1.4$ (nur CNG) auf $\lambda = 1.8$ (50 vol% H_2) und im Betrieb mit AGR von AGR = 10% (nur CNG) auf AGR ≥ 25% (50 vol% H_2) erhöht werden konnten. Die Erweiterung des Bereichs für Magerbetrieb ermöglicht eine bedeutende Reduktion der NOx Rohemissionen unter 250 mg/Nm^3, was in der Schweiz die gesetzliche Grenze für stationäre Gasmotoren der kleinsten Klasse darstellt. Im Fall des erweiterten Bereichs für Abgasrückführung kann dieser Grenzwert allerdings auch bei Zugabe von H_2 nicht erreicht werden. Die Effizienzverbesserung durch H_2-Zugabe steigt rasch mit zunehmendem λ und weist eine erkennbare Änderung ab $\lambda = 1.2$ auf. Dieses Phänomen kann für den Betrieb mit erhöhter Abgasrückrückführung kaum festgestellt werden.

Résumé

Ce projet a débuté le 1 janvier 2014 et s'est achevé le 30 septembre 2017. Le présent rapport final décrit les résultats obtenus sur l'ensemble du projet qui comportait les blocs de travail Future Mobility Demonstrator réalisé par l'Empa (BT1), méthanisation effectué par le PSI (BT2) et essais pratiques réalisé par l'EPFZ (BT3).

BT1 - Future Mobility Demonstrator de l'Empa

Dans ce premier bloc de travail, une installation Power-to-Gas avec production locale d'hydrogène a été réalisée. Cette installation comprenait les composants suivants: un électrolyseur PEM de 180 kW, une compresseur à piston de 44 MPa, un réservoir de stockage sous pression de 44 MPa et une colonne de distribution de HCNG sous une pression de 35 MPa. Cette filière hydrogène comprenant la production, la compression et le stockage réalisée au cours de l'année 2015 (mise en exploitation en novembre 2015) et la colonne de distribution d'hydrogène sous pression de 35 MPa qui est en service de depuis cette date.

De plus, un modèle Matlab de l'installation Power-tu-Gas été développé pour étudier les aspects de son dimensionnement et de l'optimisation de son exploitation pour ce qui est des coûts du courant et de la disponibilité de l'électricité renouvelable. Des mesures effectuées sur l'installation de démonstration ont servi à procéder à des analyses well-to-tank qui montrent que 57% (pouvoir calorifique supérieur) de l'énergie électrique parviennent jusque dans le réservoir du véhicule (35 MPa). Cette valeur augmente à 70% pour les installations industrielles de petites dimensions. D'autres mesures concernant la dynamique de l'électrolyseur utilisé confirment sa capacité de réagir rapidement aux variations de charge. La réaction à des de variations de charge données s'effectue en un espace de 2 seconde, voire même d'une fraction de seconde, suivant les modalités de l'induction de la variation de charge.

BT2 – Méthanisation au PSI

Le deuxième bloc de travail était consacré à l'étude et à la démonstration du stockage de pointes de courant sous forme de (bio)méthane avec le processus de gazéification et de méthanisation hydrothermal développé par le PSI. Une approche comprenait la production de H_2 par électrolyse et l'introduction de cet hydrogène avec de la biomasse dans un processus de gazéification hydrothermal. La faisabilité de cette approche a été démontrée par modélisation sur ordinateur et aussi dans la pratique avec des expériences à petite échelle sur une installation d'essai de gazéification hydrothermale en continu au PSI. L'adjonction de H_2 avec un rapport stoechiométrique à de la glycérine a permis de produire un gaz riche en méthane avec une teneur en méthane de (86 ± 6) % vol qui correspond à la valeur maximale calculée de 88 % vol à l'équilibre chimique. Une deuxième approche prévoyait de recourir pour la gazéification hydrothermale à un générateur de chaleur électrique utilisant les pointes de courant excédentaires. En absence de telles pointes, le générateur de chaleur devait pouvoir utiliser du gaz riche en méthane. A cette fin, un générateur de chaleur mixte gaz/électricité utilisant des composants disponibles sur le marché a été conçu. Il a ainsi été possible de démontrer que ces deux approches pour le stockage des pointes de courant sous forme de (bio)méthane utilisant la gazéification hydrothermale sont réalisables.

De plus, le savoir-faire technique en matière de méthanisation du CO_2 (transformation de biogaz et de CO_2 pur provenant par exemple de sources industrielles) et la méthanisation riche en H_2 de gaz fatals provenant de la gazéification a pu être amélioré. Comme l'installation pilote “GanyMeth” qui devait à l'origine être utilisée n'était malheureusement pas disponible durant ce projet, ces travaux ont été réalisés sur l'installation “Cosyma” (TRL 5).

Dans le cadre d'un autre projet, "Cosyma” a été raccordée à une installation de production de biogaz à Zurich. Une fois les objectifs de ce projet atteint, l'exploitation de l'installation a été poursuivie pour réaliser des expériences d'optimisation. Lors de ces expériences on constaté que l'adjonction d'eau pouvait être notablement diminuée sans qu'il se forme de coke, ce qui améliore le rendement du réacteur principal et permet de réduire les dépenses (CAPEX et OPEX) pour l'étape préparatoire du processus.

Parallèlement à cela, on a procédé à la modélisation et à l'optimisation de la chaîne complète du processus Power-to-Gaz basée sur le biogaz. Pour cela, les unités principales (réacteurs, membranes) ont été représentées à l'aide de modèles de non-équilibre alors que les autres unités du processus ont été représentées à l'aide de modèles thermodynamiques et short-cut. La description détaillée de quatre concepts de processus différents a permis de réaliser des calculs des coûts précis. Il est apparu que, du fait des spécifications pour l'injection dans le réseau, une étape de préparation – p.ex. à l'aide de membranes de séparation de H_2 ou d'un réacteur à lit solide placé en amont – était nécessaire. L'utilisation d'une membrane séparatrice de H_2, qui à son tour modifiait les conditions dans le réacteur principal du fait de la réutilisation de cet hydrogène, s'est révélée optimale sur le plan de la stabilité et de la flexibilité du processus.

BT3 - essais pratiques de HCNG à l'EPFZ et à l'Empa.

Le troisième bloc de travail était consacré à des études sur l'utilisation du mélange de carburant HCNG sur des installations mobiles et stationnaires. Le HCNG contient de l'hydrogène (H_2) et du gaz naturel/biogaz (CNG, pour "compressed natural gas"); dans ces études l'accent portait sur une adjonction de 0 à 25 % vol de H_2 pour les applications mobiles et de 0 à 50 % vol. de H_2 pour les applications stationnaires.

Pour permettre le ravitaillement en carburant de trois véhicules CNG on a réalisé dans un premier temps une solution de ravitaillement provisoire qui permettait une adjonction basse de 2 % vol de H_2. Ces 2% vol correspondent à la proportion maximale de H_2 admise pour les véhicules CNG conventionnels selon les prescriptions suisses. Les véhicules tests ont été exploités durant plusieurs mois avec du CNG pur et avec une adjonction de 2 % vol de H_2 au sein de la flotte des véhicules de livraison des paquets de la poste suisse. Les données de mesure ont été recueillies à l'aide d'appareils d'enregistrement embarqués.

L'analyse de ces données a montré une légère tendance à une amélioration de l'efficience et à la diminution des émissions de CO_2 très probablement dues à l'amélioration du processus de combustion. La quantité de H_2 ajoutée était toutefois très faible, de sorte que cet effet se situe dans le domaine de l'incertitude statistique. On a toutefois pu constater que le comportement du moteur était notablement amélioré.

D'une manière générale on a pu confirmer que l'adjonction de faibles quantités de H_2 au carburant de véhicules CNG conventionnels n'a pas un effet négatif mais bien un effet positif, et cela bien qu'aucune modification n'ait été apportée à ces véhicules. Une publication sur ce thème, actuellement en cours de rédaction, devrait paraître début 2018.

Pour les essais pratiques avec une adjonction plus élevée de H_2 (jusqu'à 25 % vol) un autre véhicule CNG a été modifié, avec un nouveau réservoir et de nouvelles conduites de carburant, afin d'assurer sa compatibilité avec H_2. Le nouveau système de carburant et le véhicule dans son ensemble ont été re-certifiés et le véhicule a débuté ses essais pratiques dans la flotte de véhicules de livraison des paquets de la poste suisse. Parallèlement à cela on a réalisé une solution permanente pour le ravitaillement des véhicules en HCNG permettant une adjonction de 0 à 30 % vol. de H_2. La construction et l'algorithme de commande de cette colonne de ravitaillement en HCNG ont été développés à l'Empa et reposent sur des mesures et des simulations qui ont été réalisées dans le cadre de ce projet. Durant ces essais pratiques, on n'a constaté aucun effet négatif aussi bien pour l'exploitation CNG que pour l'exploitation HCNG et la colonne de ravitaillement HCNG a fonctionné aussi fiablement qu'une colonne CNG conventionnelle.

Pour ce qui est des installations stationnaires, on a étudié l'influence du HCNG sur une micro-centrale de cogénération. Ici l'accent portait sur l'analyse des effets de l'adjonction de H_2 sur le processus de combustion et sur les émissions brutes en fonctionnement en mélange pauvre et avec recirculation des gaz d'échappement (RGE). Les mesures ont été réalisées sur un moteur atmosphérique 4 temps monocylindre à allumage commandé d'une cylindrée de 250 cm^3. Le banc d'essai comprenait une unité de mélange des gaz en amont qui alimentait le moteur avec des quantités définies de gaz recirculés et d'hydrogène.

Il est apparu que l'adjonction de H_2 permettait d'augmenter les limites d'exploitation d'une micro-centrale de cogénération avec moteur atmosphérique en fonctionnement en mélange pauvre de $\lambda = 1.4$ (CNG seul) à $\lambda = 1.8$ (50 vol% H_2) et en exploitation avec gaz recirculés de RGE = 10% (CGN seul) à RGE ≥ 25% (50 % vol. H_2). L'élargissement du domaine de fonctionnement en mélange maigre permet une réduction importante des émissions brutes de NO_x à des valeurs inférieures à 250 mg/Nm^3 qui est la valeur limite fixée par la législation suisse pour les moteurs à gaz stationnaires de la plus petite classe. Dans le cas de l'élargissement du domaine en régime pauvre avec recirculation des gaz d'échappement, cette valeur ne peut pas être atteinte, même avec une adjonction de H_2. L'amélioration de l'efficience provoquée par l'adjonction de H_2 s'accroit rapidement avec l'augmentation de λ, avec un changement décelable à partir de $\lambda = 1.2$. Un phénomène qui n'est guère décelable lors de l'exploitation avec un accroissement de la recirculation des gaz d'échappement.

Summary

The project started on the 1st of January 2014 and was finished per 30st of September 2017. This final report is showing the achievements over the whole project. The project is divided into the work packages Future Mobility Demonstrator at Empa (WP1), Methanation at PSI (WP2) and HCNG field testing at ETHZ and Empa (WP3)

WP1 - Future Mobility Demonstrator at Empa

In WP1, a Power-to-Gas facility was realized with local hydrogen production by a 180 kW PEM electrolyzer, a 44 MPa piston compressor with 44 MPa pressure cylinder storage as well as a 35 MPa H_2 fueling station and a 35 MPa HCNG fueling station. The onsite H_2 production and fueling hardware was installed in 2015 (with inauguration in November 2015) and the 35 MPa H_2 fueling station is in operation since then.

Beside this, a Matlab model of the Power-to-Gas facility was developed which allows investigating design aspects or optimized operational strategies with respect to electricity costs and availability of renewable electricity. On the basis of measurements on the demonstrator, well-to-tank analyses were conducted showing that 57% (HHV) of the electrical energy reaches the vehicle tank (35 MPa). This figure increases to 70 % (HHV) for small industrial scale facilities. Further measurements regarding the dynamics of the employed PEM electrolyzer confirm the ability of rapid load changes to be within 2 seconds or even tenths of seconds depending on the way the load changes are induced.

WP2 – Methanation at PSI

In WP2, peak electricity storage as (bio-)methane was studied and demonstrated using the hydrothermal gasification and methanation process developed at PSI. One approach involved the production of H_2 by electrolysis and co-feeding the H_2 with the biomass into the hydrothermal gasification process. The feasibility of this approach was demonstrated both theoretically by modeling as well as by small-scale experiments in a continuous hydrothermal gasification test rig at PSI. Addition of hydrogen in a stoichiometric amount produced a methane rich gas from glycerol with (86 ± 6) vol% CH_4, which corresponded to the calculated maximum value of 88 vol% at the chemical equilibrium. No detrimental effect on the catalyst when co-feeding H_2 was observed. A second approach would involve an electric process heater for the hydrothermal gasification process, operated on the peak electric power. When no such peak power is available, the heater would be operated on a methane-rich gas. To this aim, a dual gas/electric heater was designed using commercial components. In summary, both approaches to store electric peak power as biomethane using hydrothermal gasification technology were shown to be feasible.

In addition, the know-how on CO_2 methanation (converting biogas and pure CO_2, e.g. from industrial sources) and hydrogen-rich methanation of gasification derived producer gas was increased by modelling and experiments. As the pilot scale set-up “GanyMeth” that originally should be used unfortunately was not available within the project time, experiments were conducted using the TRL 5 plant Cosyma.

Within another project, Cosyma was connected to a biogas plant in Zürich. After achieving the goals of that other project, the operation of the installation was continued to conduct optimization experiments. In these experiments, it was found that the addition of water can be significantly reduced without coke formation, which improves the yield in the main reactor and will allow decreasing the effort (CAPEX and OPEX) in the upgrading step of the process.

In parallel, the complete process chain of biogas based PtG was modelled and optimized. For this, the main units (reactors, membranes) were represented by rate-based models, while other process units were calculated with thermodynamic and short-cut models. The detailed description of four different process concepts allowed also detailed cost calculations. It was found that the grid injection specifications make an upgrading step, e.g. by a hydrogen separation membrane or a second fixed bed reactor, necessary. The optimum with respect to process robustness and flexibility turned out to be introducing a hydrogen separation membrane which in turn changed the conditions in the main reactor due to recycled hydrogen and methane.

WP3 - HCNG field testing of ETHZ and Empa

In WP4 investigations on the utilization of the fuel mixture HCNG for mobile and stationary applications were carried out. HCNG contains H_2 (hydrogen) and CNG (natural gas/biogas) whereby the focus lied on H_2 admixture of 0 to 25 vol% for the mobile and 0 to 50 vol% for the stationary application.

To enable refueling of three CNG test vehicles, a temporary refueling solution allowing low H_2 admixture of 2 vol% was realized firstly. 2 vol% is the permitted H_2 fraction for conventional CNG vehicles by the respective Swiss regulations. The test vehicles were operated several months with both pure CNG and 2 vol% H_2 admixture as part of the parcel delivery fleet of Swiss Post while data was gathered onboard with data loggers. The analysis of the data indicated small tendencies towards improved efficiency and a decrease in CO_2 emissions which presumably results from an improved combustion process. The amount of H_2 added was very little, the effect lies within the statistical uncertainty. However, it was observed that engine starting behavior could be improved considerably. In general the results confirmed that adding low amounts of H_2 in the fuel of conventional CNG vehicles have no negative but rather positive effects even though no modifications to the vehicle were carried out. A paper on this topic is currently in preparation and is expected to be submitted in the beginning of 2018.

For the field tests with higher H_2 content (up to 25 vol%) a different CNG vehicle was retrofitted with new tanks and fuel lines to ensure compatibility with H_2. The new fuel system and the vehicle have been re-certified and the vehicle has started its field test in the parcel delivery service of Swiss Post. Also a new permanent HCNG dispenser was realized allowing the refueling of mixtures with 0 to 30 vol% of H_2. The setup and the control algorithm of the dispenser were developed at Empa based on measurements and simulations carried out in the scope of this project. During the field test, the vehicle showed no negative behavior, neither in CNG nor in HCNG operation and also the HCNG filling station worked as reliable as the normal CNG filling station.

Regarding stationary applications the impact of the fuel HCNG on a micro combined heat and power plant (mCHP) was investigated. Thereby the emphasis was put on analyzing the effects of exhaust gas recirculation (EGR) and H_2 admixture on the combustion process. Measurements were taken on a single cylinder 4-stroke spark ignited and naturally aspirated engine of 250 cm^3 swept volume including an upstream gas mixing device to supply predefined rates of EGR and H_2.

It was found that by adding H_2 to CNG it is possible to extend the operating limits of a naturally aspirated mCHP engine for lean burn operation from $\lambda = 1.4$ (CNG only) to $\lambda = 1.8$ (50 vol% H_2) and for EGR operation from EGR = 10% (CNG only) to EGR ≥ 25% (50 vol% H_2). The extension of the operating lambda allows for a significant raw NOx emission reduction down to below 250 mg/Nm^3 which is the legal limit for stationary gas engines in the smallest power class in Switzerland. However, even with hydrogen extended EGR operation this NOx limit cannot be reached. The efficiency bonus of adding hydrogen increases rapidly with increasing lambda and can be observed starting from $\lambda = 1.2$. This phenomenon is almost not observable for EGR operation.

Content

Abbreviations

CHM	Catalytic Hydrothermal Methanation
CIGS	Copper Indium Gallium Selenide solar cell
CNG	Compressed Natural Gas (komprimiertes Erdgas/Biogas)
CTFF	Crank Time First Firing
COV	Coefficient of Variation
DPM	Dynamic Programming Method
ECU	Electronic Control Unit
ehub	Energy distribution concept of NEST building at Empa
EGR	Exhaust Gas Recirculation
Empa	Swiss Federal Laboratories for Material Science and Technology
ETH	Swiss Federal Institute of Technology
FTIR	Fourier Transformation Infrared Spectroscopy
HCNG	Wasserstoffangereichertes Erdgas/Biogas
HTG	Hydrothermal Gasification process
IMEP	Indicated Mean Effective Pressure
MS	Mass Spectrometry
mCHP	micro Combined Heat and Power plant
NEST	Future building demonstrator at Empa
PEM	Proton Exchange Membrane
PLC	Programmable Logic Controller
PSI	Paul Scherrer Institute
PVT	Pressure Volume Temperature
SFOE	Swiss Federal Office of Energy
STVA	Strassenverkehrsamt
SQL	Structured Query Language
SVGW	Schweizerischer Verein des Gas- und Wasserfaches
TPO	Temperature Progrmmed Oxidation
TRL	Technology Readyness Level

1. Future Mobility Demonstrator at Empa (WP1)

1.1. General targets and state of WP1 compared to the proposal aims/milestones

In accordance with the project objectives a demonstration plant was realized, which shows how excess or unprofitable electricity can be stored in chemical form and utilised in the mobility sector. The building containing the plant was designed according to safety regulations and renovated in 2014. In the same year the dimensioning of the plant was completed based on simulations and the orders for the main components were placed. By the end of 2014 the electrolyser was delivered. In the course of 2015 all remaining components for production, compression, storage and dispensing of H_2 at the standard pressure of 35 MPa were delivered.

In 2016 a model of the demonstration plant was developed within the scope of a semester project in collaboration with ETH Zürich. For validation purposes a first measurement series was carried out. On the basis of a second measurement series in 2017 well-to-tanks analysis as well as investigations regarding electrolyzer dynamics were conducted.

1.2. Main achievements

The following listing summarizes the main achievements within WP1 throughout the complete project duration.

- Working Power-to-Gas demonstration plant *move* including components for H_2 production, compression, storage and dispensing at 35 MPa
- Installed overall control system for data recording and plant operation according to electricity prices and availability of renewable electricity
- Modell and simulation results for the demonstration plant in terms of price-optimized operation strategies
- Measurements of real-world energy consumption from H_2 production to H_2 fueled in vehicle tank at 35 MPa (well-to-tank)
- Measurements of electrolyzer dynamics

Subsequently, these achievements are elaborated.

<u>Power-to-Gas demonstration plant “move”</u>

Within the scope of this project the main components of the demonstration plant *move* were dimensioned, acquired and installed. The schematic below shows the plant setup with the previously existing CNG pathway (green) and the newly realized H_2 pathway (blue) in bright color. The plant includes a dispenser for HCNG (mixture of H_2 & CNG) and H_2 at a pressure level of 35 MPa. Faded symbols represent plant extensions which are part of related projects whereby the pathway for H_2 refueling at 70 MPa has already been realized as well.

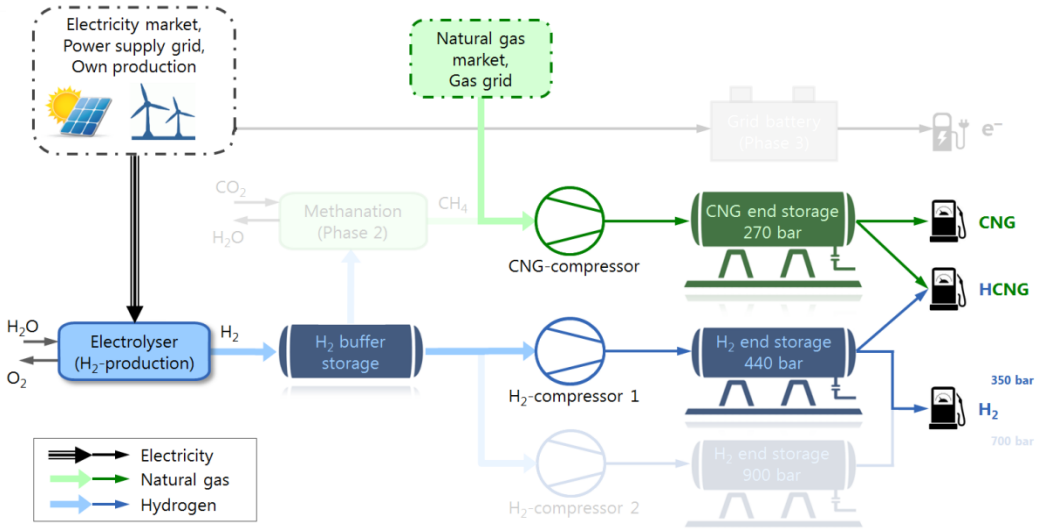

Fig. 1 Schematic of the demonstration plant "*move*"

Electricity is supplied on one hand by photovoltaic panels on the roof and the façade of the building adjacent to the demonstration plant. The cumulated peak power of the panels amounts to 70 kW_p. Next to conventional multicrystalline panels also panels on the basis of the CIGS technology were installed which are manufactured by the ETH/Empa spin-off *Flisom*. Through this thin film technology utilization of energy and cost intensive materials can be reduced significantly. Further, electricity is supplied from a running river power plant with documented proof of origin.

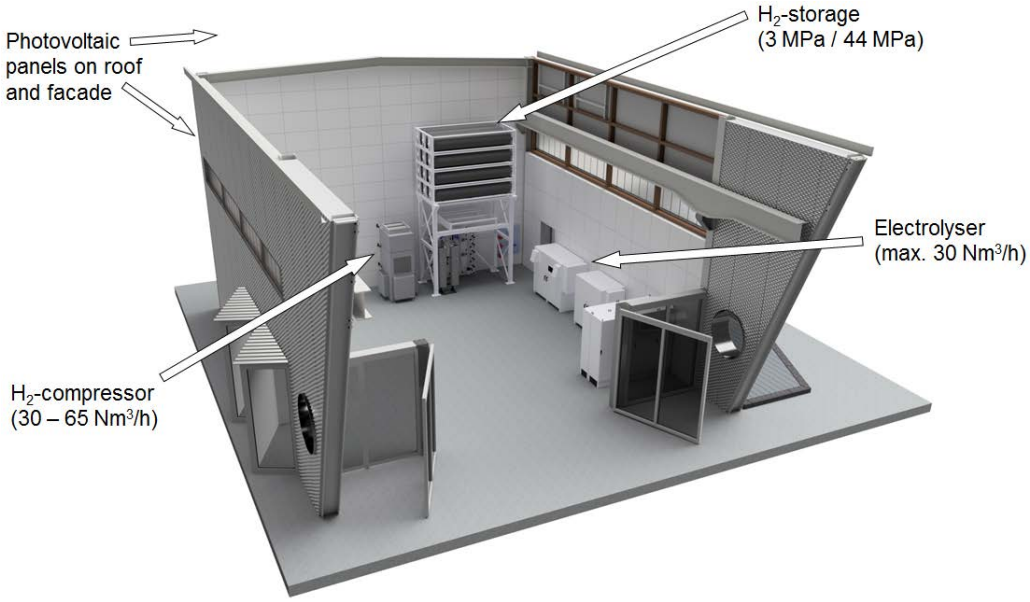

Fig. 2 Components of the demonstration plant move installed within the scope of this project

The renewable electricity is used within the electrolyzer to split up water into H_2 and O_2 whereby a H_2 production rate of 30 Nm^3/h is reached at full load. As PEM technology is employed for the electrolysis, load changes introduced by fluctuating electricity sources can be followed very rapidly (see section “Electrolyzer dynamics”). To increase flexibility a buffer storage (3 MPa) is installed downstream of the electrolyzer allowing to store the generated H_2 of three hours in full load operation. Using a four stage piston compressor H_2 is then brought to a pressure level of 44 MPa and stored in the end storage tanks. The H_2 and the HCNG dispenser on the north-eastern façade of the building enable refueling from these tanks by employing cascade-type refueling.

Inherently, challenges regarding plant realization were related to project management. Due to project partnerships as well as suppliers specializations the necessary plant components were delivered by different suppliers. Clarifying interfaces and coordination, therefore, demanded significant efforts on the side of Empa to enable successful system integration. Furthermore, various preparation works were necessary onsite. Namely the cooling system for the electrolyzer including pump, heat exchanger and piping as well as underground piping for H_2 and electrical lines beneath the fueling station were installed beforehand. The pictures below present an example of preparation work in the form of a steel framework and gas vessel mounting racks which were designed at Empa and fabricated by an external supplier.

Fig. 3 Installation of the rack mounted end storage tanks onto the steel framework (left) and the demonstration plants exterior view by night (right)

During the planning and installation phase regular contact to authorities was maintained to ensure the demonstrator was built according to valid regulations. Experiences gained regarding this topic are collected and will be made available for future plant designer and operators.

With the realization of the demonstration plant *move* a platform was created for various research endeavors in the area of production and refueling of renewable synthetic fuels. Having the possibility for investigations under real-world conditions is a valuable asset for current and future projects in this area.

Overall control system

To provide a common location for data recording from all components of the demonstration plant, a PLC from Beckhoff Automation was installed. On one hand data is read out directly from the PLC via USB-stick. On the other hand, the PLC writes data to a SQL database which stores all measurements to be easily accessible for later use. Other energy-related demonstration projects of Empa (*e-hub*, *NEST*) write data to the same database utilizing the same coding system.

The Beckhoff-PLC is also used for overall control of the plant. Whereas each single component has its own control, their commands may be overwritten via the Beckhoff-PLC to follow a predefined operation strategy. For instance, the elctrolyzer is started by its control whenever pressure in the downstream buffer storage drops. The same holds for compressor and end storage tanks, whereby the compressor control follows a specified hysteresis. Through the Beckhoff-PLC, start and stop as well as the load setting of electrolyzer and compressor can be controlled taking into account electricity prices and availability of renewable electricity.

Model for price-optimized operation:

Within the scope of a semester project in cooperation with ETH a model of the demonstration plant was developed in Matlab. The individual components were modeled using discretized differential equations for mass and energy and the equation of state for real gases. Unknown constants were estimated based on literature data in a first step and validated with measurements conducted on the demonstration plant. Following screenshot of the end storage tank program block is intended to give an idea of the model interface.

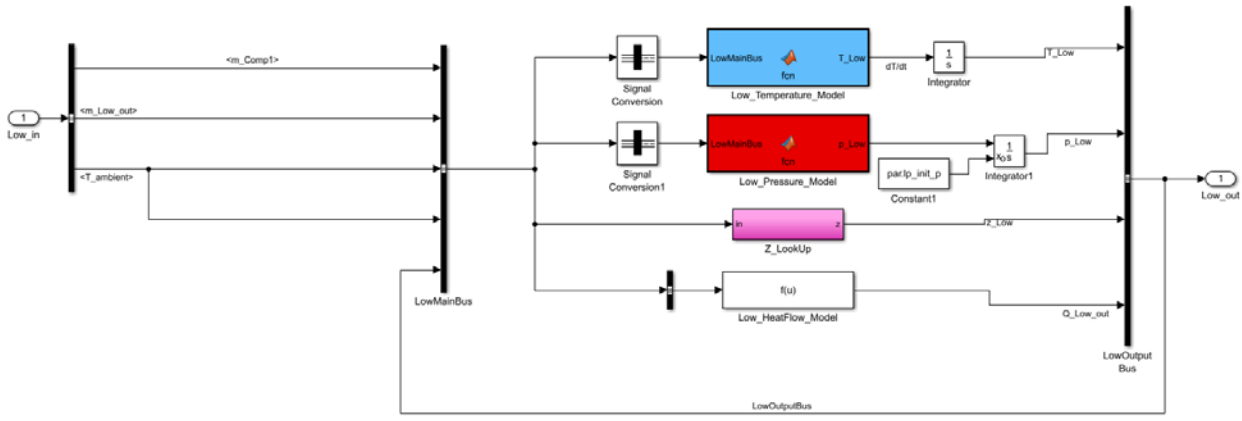

Fig. 4 Matlab Simulink interface for a component (end storage tank) of the demonstration plant model

In general it will be possible to use the model for various investigations regarding the plants behavior. In subsequent consideration, the focus lies on finding a price-optimized operation strategy for the plant. The input parameters below were predefined:

- Electricity spot price (SWISSIX EPEX Spot Hour Prices 2015, first 20 days in January)
- Demand at refueling station (Scale up of measured demand)
- Ambient temperature

In a first step, a rather straightforward strategy was followed, in which the plants components are only operated when the electricity price drops below a certain price limit.

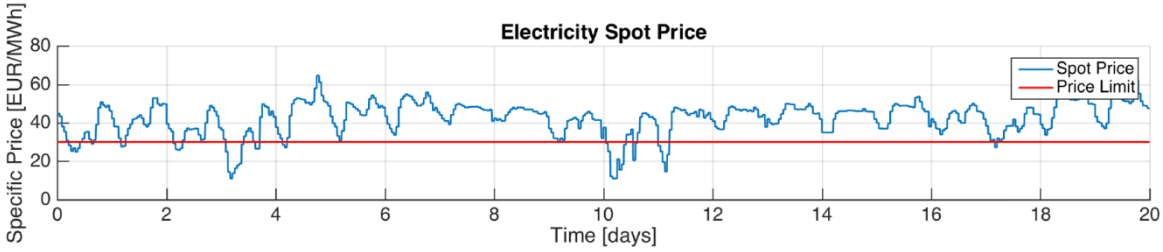

Fig. 5 Electricity spot prices at SWISSIX EPEX in January 2015 (blue) and an exemplary price limit of 30 EUR/MWh

The value of this price limit is influenced by abovementioned input parameters as well as the constraints set within the model. For instance, the minimal pressure setting for the end storage tanks represents such a constraint. In this case the pressure setting is chosen such that the tank always contains enough H_2 to refuel at least one vehicle. If the constraint is violated, the tanks are filled immediately even if the current electricity price lies well above the predefined limit. Therefore, if price limit is set too low, the components will potentially run when electricity prices are high. The diagram below shows, that the specific production costs were lowest when the price limit was set in the order of 30 EUR/MWh with the selected input parameters. Obviously, depending on the plant and the input parameters this value will change.

Using a more sophisticated approach which avoids the orientation on a fixed price limit, the specific costs can be lowered further. For that purpose a mathematical optimization method called “dynamic programming” (DPM algorithm) was employed. In this method solutions for the smallest subproblems are computed first and then combined to solve the next larger problems until a solution to the overall optimization problem is reached. The following diagram shows the specific costs when the plant is operated according to the strategy based on the DPM algorithm (yellow) in comparison with different price limit strategies.

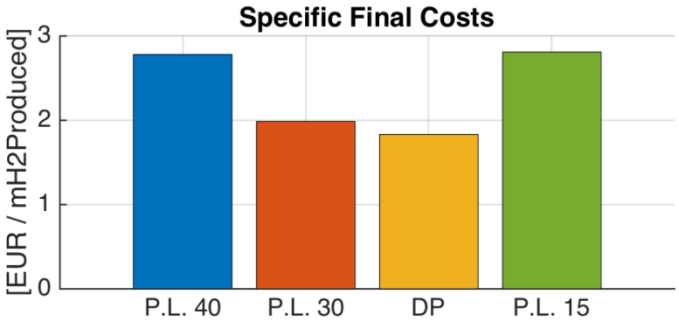

Fig. 6 Specific final costs per generated mass of H_2 employing different operational strategies

Note that the shown simulation results to find optimal operational strategies are based on a known electricity price for a given period. To determine how to actually operate such a plant for the present and upcoming days electricity price forecasts are of importance. The more accurate the forecasts, the higher is the optimization potential of the operational strategy using abovementioned methods.

In a further remark, periods of low electricity prices correlate very well with periods of high renewable electricity shares in the power grid. This means that an economically viable strategy will inherently lead to a favorable electricity demand with respect to time.

Well-to-tank analysis

Based on several measurement series on the electrolyzer and the compressor of the demonstration plant the energy losses along the pathway of H_2 production to refueled H_2 at 35 MPa were determined. The energy flows are visualized in the Sankey diagrams below whereby diagrams on the left and on the right are based on the lower heating value (LHV) and the higher heating value (HHV) of H_2, respectively. The bottom diagrams represent conversion efficiencies for components used in small industrial scale plants with an electrical input in the low MW-range. For better comparison, both demonstration plant and industrial scale plant comprise of the same components. Note, however, that industrial size plants might not produce H_2 onsite so that energy for transport would need to be considered as well.

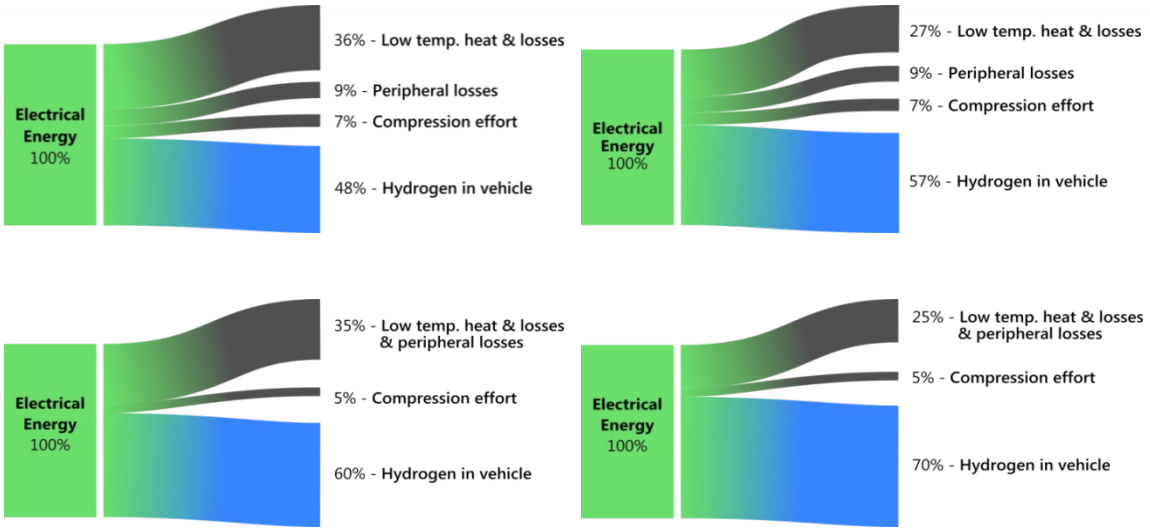

Fig. 7 Well-to-tank analysis for the plant move (LHV: top-left / HHV: top-right) and an industrial size plant (LHV: bottom-left / HHV: bottom-right)

Data for industrial scale plants were provided by manufacturers of the respective components and could not be confirmed with own measurements. However, the previously provided data for the components of the demonstration plant correlated well with own measurements, so that the given numbers are expected to be feasible.

The energy share ‘Low temperature heat & losses’ represents predominantly the heat produced by the cell stacks of the electrolyzer which is carried away by the coolant. The temperature level of the coolant at the exit of the electrolyzer amounts to around 55 - 60°C. At the demonstration plant *move* this heat is passed on to Empa’s heat network and supports the existing heating system in the winter half-year. For the electrolyzer of the move plant, non-stack related losses are shown separately as ‘Peripheral losses’. These losses include for instance the energy expended for circulation pumps, fans, control units and rectification. A substantial amount of energy, however, is needed for the drying of H_2. In case of the industrial plant, the share of low temperature heat and peripheral losses are summarized in one branch.

The share ‘Compression effort’ shows the amount of energy needed to compress H_2 from 0.5 to 44 MPa. This allows vehicle refueling to a nominal pressure of 35 MPa which is standard for H_2 utility vehicles. The specific compression energy for the industrial scale plant is based on an ionic compressor.

Note that the numbers stated in the Sankey diagrams represent the point of maximum efficiency which is reached in the region of 30 – 50% of maximum H_2 production. For lower or higher production rates the share of the losses increase. However, for the wide range of around 15 – 100% of production capacity the conversion efficiency only deviates by a few percentage points from the maximum value.

To attain the energy shares for the *move* plant, the electrical input to the electrolyzer was measured with a power meter while the H_2 output was recorded using a Coriolis sensor. As the rectification and drying equipment is part of the electrolyzer unit, all peripheral losses are included in above numbers besides the energy needed for cooling. Cooling water is supplied by the Empa cooling network. However, according to data from manufacturers cooling energy demand is very low and would increase peripheral losses only by a small amount.

The energy consumption of the compressor was measured using a power meter as well, whereas the H_2 throughput was determined on the basis of pressure measurements in the storage tanks and the PVT method (pressure, volume, temperature). The electrical energy needed per energy which is contained in the compressed H_2 was observed to be around 24% as opposed to 15% which was measured by the manufacturer and project partner Atlas Copco. An examination of the compressor showed, that, presumably, internal leaks led to the decrease in throughput which caused the increased specific energy consumption. Atlas Copco is still gathering experiences regarding the practical operation of their H_2 compressor and can use the demo plant *move* as a platform to improve their product. For the diagrams and the table above the numbers measured by the manufacturer were inserted as these are expected to be achieved with a properly working piston compressor.

The conversion efficiencies of the individual components are summarized in the table below.

Tab. 1 Electrolyzer efficiency (top) and normalized energy consumption of compressors (bottom)

Electrolyzer (including peripheral losses and H_2 purification) Type: PEM	**Efficiency based on LHV [%]**	**Efficiency based on HHV [%]**
Demo plant move (measured, confirmed)	52	61
Industrial scale components	63	74

Compressor Input pressure: 0.5 MPa Output pressure: 44.0 MPa	**El. energy needed per energy in compressed H_2 (LHV) [%]**	**El. energy needed per energy in compressed H_2 (HHV) [%]**
Demo plant move (measured, *not* confirmed) (4-stage piston compressor)	15	13
Industrial scale components (ionic liquid compressor)	8	7

Electrolyzer dynamics

The electrolyzer employed at Empa has two types of stand-by modes which mainly differ in power consumption and load change ability. In the ‘idle mode’ electricity is applied to the stacks, whereas in the ‘shut-off mode’ only few peripheral appliances and the control unit are running. The diagram below shows the evolution of electrical power input as well as the exiting H_2 mass flow. The electrolyzer was started from ‘shut-off mode’ with all internal components being at ambient temperature of 17°C.

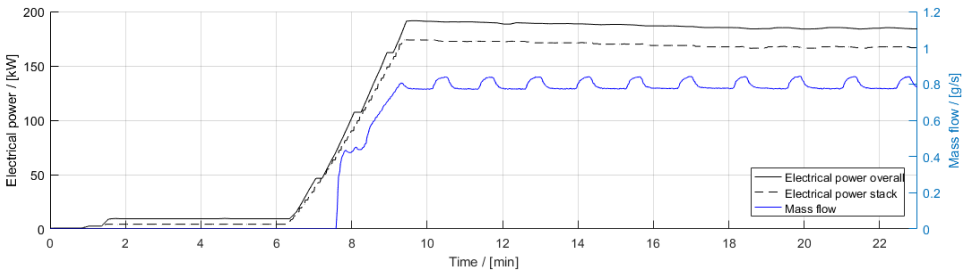

Fig. 8 Evolution of overall power and stack power as well as H2 mass flow when starting the electrolyzer from ‘shut-off mode’

After starting the electrolyzer at t = 0 min, built in tests are executed and the coolant circulation pump starts running. At around 1.5 min current is applied to the stacks and H_2 is generated at a very low rate. As the purity of the produced H_2 is not according to specifications during this start-up phase it is released through the vent to the atmosphere during several minutes. After approximately 6.5 min the current applied to the stacks is increased following a predefined ramp curve and pressure is build up to 3 MPa. At around 7.5 min H_2 mass flow is detected at the exit of the electrolyzer and rises to its full load value after approximately 9 min.

Note how overall power (solid line) and stack power (dashed line) slightly decrease by 7 kW during 9 min (from 9 to 18 min) after reaching full load. With increasing stack temperature reaction kinetics improves and conversion efficiency rises by a few percentage points leading to the lower power demand. Regarding H_2 mass flow a periodic increase can be observed which is caused by the regeneration of the pressure swing adsorption unit (drying unit).

If the elctrolyzer is not completely shut-off, but put into ‘idle mode’, full load is achieved much more rapidly. The measurements for the following diagram were recorded after the electrolyzer had reached its operating temperature. By closing a hand valve at the outlet, the elctrolyzer was put into ‘idle mode’. At t = 5 s the valve vas instantly opened and stack current increased within less than 2 s to full load. As the resolution of the mass flow measurement cannot be set higher than around 0.7 Hz its values are visualized with markers instead of curves. The mass flow overshoots after opening the valve as pressure has built up before the valve when it was closed. Subsequently it drops to the value measured at full load under stationary conditions.

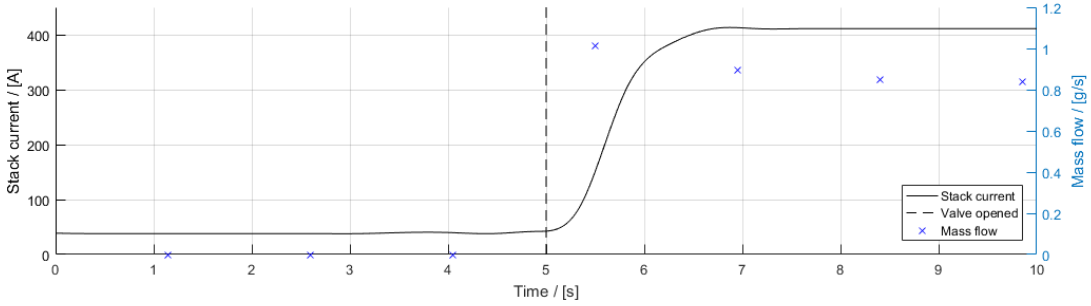

Fig. 9 Evolution of stack current and mass flow when changing from zero to full load by operating a hand valve at the exit of the electrolyzer

As the illustrated load change was generated by operating a valve at the outlet it is only representative for storage pressure induced load changes. However, a load change can also be induced by altering input electricity of the electrolyzer which is not possible with the current setup at the *move* plant. Input electricity induced load changes are expected to be significantly faster so that a load change from zero to full load is possible within tenths of seconds.

Naturally, changes to or in between intermediate loads are achieved even more quickly. Measurements regarding negative load changes (e.g. from full load to zero) showed very similar temporal behavior. If the electrolyzer is completely shut-off the shutdown procedure takes around 2 min. When it is started from 'shut-off mode' immediately after shutdown, full load is reached after approximately 6 min instead of abovementioned 9 min.

The following table summarizes the power consumption and the load change ability for the described stand-by modes. When ambient temperature drops below 5°C electrical heaters are started within the electrolyzer enclosure to prevent freezing conditions which could damage the stacks. Those heaters maximally take up 2.1 kW of electrical power.

Tab. 2 Power consumption and load change ability for the stand-by modes

Stand-by mode	Power consumption [kW]	Approx. time to full load [s] (Electrolyzer at amb. temp.)	Approx. time to full load [s] (Electrolyzer at operating temp.)
Shut-off	0.7 (+2.1)	540	360
Idle	13	-	2 / tenths of seconds

1.3. Dissemination activities within the WP1

13.05.14	Expertengespräche „Applied Power-to-Gas“ at HSR in Rapperswil Oral presentation introducing the demonstration plant “move” and the activities of the project.
25.02.15	Event “Power-to-Gas in der Mobilität” at Empa Including presentation and guided tour through demonstration plant “move” and introduction of the activities of the project.
18.06.15	POSTER: “Parlamentarieranlass” in front of the Bundeshaus in Bern
03.07.15	European Fuel Cell Forum EFCF in Luzern Oral presentation on the demonstration plant “move” and activities of the project.
25.08.15	Event “Energiewende – smart und innovativ” of Ökostrom Schweiz at Empa Oral presentation on the demonstration plant “move” and activities of the project.
26.08.15	POSTER: “2nd annual SCCER mobility conference” at ETHZ
28.10.15	Gasmobil Symposium at Empa Dübendorf Oral presentation on PtG and the demonstration plant move: “CO_2-neutral dank Power-to-Gas”
19.11.15	Werkleiterseminar Gasversorgungsunternehmen in Brunnen Oral presentation on PtG and the demonstration plant move: “CO_2-neutral dank Power-to-Gas”
23.11.15	Official inauguration of the demonstration plant “move” The inauguration was led by various talks given by Brigitte Buchmann (Head of the Department Mobility, Energy and Environment and a member of Empa’s Board of Directors), Gian-Luca Bona (Director of Empa), Walter Steinmann (Director of the Swiss Federal Office of Energy (SFOE)), Lothar Ziörjen (Mayor of the energy city Dübendorf), Hans Magits, (Chief Technical Officer at the compressor manufacturer AtlasCopco) and Prof. Konstantinos Boulouchos (Prof. at the Institute for Energy Technology at ETH Zurich).

Subsequently the demonstration plant, its refueling station and various project vehicles were demonstrated to the present energy and mobility experts.

https://www.empa.ch/de/web/s604/move-inauguration

Inauguration of the plant “move” including a demonstration of hydrogen refueling

Since end of 2015 the move-webpage is active:
https://www.empa.ch/web/move

26.01.16	Event “Brennstoffzellen in automobilen Anwendungen” at Empa Including presentation and guided tour through demonstration plant “move” and introduction of the activities in the RENERG2-project.
18.08.16	Open house Day at Empa St.Gallen. Multi-day poster session Introducing the demonstration plant “move” and the activities in the RENERG2-project
15./16.09.16	2-day conference: 11. Tagung Gasfahrzeuge | Gasantriebe und Klimaschutzziele: der richtige Weg! - in Potsdam. Oral presentation on the demonstration plant “move” and activities in the RENERG2-project.
26.-30.04.17	Swiss Mobility Days in Martigny Oral presentation on the demonstration plant “move” and activities of the project.

31.08.17 move visualization – link published

Using 3D models of the building and the plants components a visualization tool of the demonstration plant was developed. The overall process as well as the individual components are animated and explained in short video sequences. Specifications of the components as well as selective real time data is also available.

The visualization can be accessed via a touch screen onsite or via the link of the move webpage: https://www.empa.ch/web/move

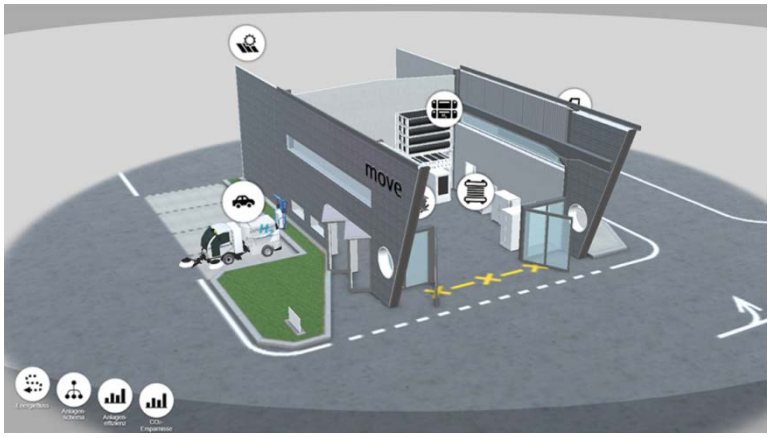

02.10.2017 Inauguration of the ‘Erlebnisstation’ realized for the ‘Umweltveloweg’

The ‘Erlebnisstation’ essentially contains a large-sized book which explains the mobility concepts investigated in the move project in a simple way. It was created to address children and families. The move visualization screen is located directly adjacent to the ‘Erlebnisstation’ in front of the move.

Throughout the duration of the project the demonstration plant was visited by many experts particularly from the energy and mobility industry. The plant was also shown to other interested parties such as individuals from politics or authorities.

1.4. Publications / patens

Publication is in preparation

1.5. Industrial and institutional WP1 partners

- SFOE — Swiss Federal Office of Energy
- ETH Board — Strategic management of ETH domain
- Glattwerk — Energy provider (electricity, natural gas/biogas)
- FOGA — Research, development and promotion fund of the Swiss gas industry
- Atlas Copco — Industrial (gas) company
  Support regarding the development of the HCNG dispenser. Extended collaboration within the project “Future Mobility Demonstrator” which is linked to RENERG^2 project WP4
- Endress+Hauser — Instrumentation and process automation company
  Collaboration in the field of mass flow metering (Coriolis). A substantial part of gaseous fuel dispensing.

2. Methanation

2.1. General targets and state of WP2 compared to the proposal aims/milestones

a) *Hydrogen addition to hydrothermal gasification/methanation*

Catalytic Hydrothermal Methanation (CHM) of wet biomass is an efficient process developed at PSI during the last fifteen years. The product gas contains ca. 54 vol% CH_4, 40 vol% CO_2, and 5 vol% H_2, as well as ca. 1 vol% of C_{2+}. Its thermal process efficiency “biomass to biomethane” in autothermal operation reaches 60 - 70%, depending on the feedstock composition. The key element of this process is a ruthenium-based catalyst that is able to decompose the larger organic molecules to small fragments and to reform them to the gases CH_4, CO_2, and H_2. Addition of H_2 to the process should shift the product composition towards more methane and less CO_2, as the CHM process is mostly conducted close to the thermodynamic equilibrium, at around 450°C and 28 MPa. Our contribution in this project was (i) to perform process simulations with added H_2, (ii) to validate these simulations by experiments in an existing continuous test rig using a model solution, and (iii) to propose a concept for a process heater for the hydrothermal gasification suited for dual operation on both natural gas and electricity.

All three deliverables/milestones were completed, although somewhat delayed compared to the original research plan. In 2016 we successfully performed an experimental campaign with our test rig KONTI-C, upgraded for the addition of pressurized hydrogen (see section below and Reimer et al., 2017 for details).

Simulations of the hydrothermal gasification process with added H_2 were performed with the software package Aspen plus and documented both in Reimer et al., 2017 and in Vogel, 2017. A concept for a dual natural gas/electricity process heater was proposed using commercial components (see section below).

b) *Hydrogen-rich methanation of CO_2-containing gases*

The goal of the activities was to increase know-how on CO_2 methanation (converting biogas and pure CO_2, e.g. from industrial sources) and hydrogen-rich methanation of gasification derived producer gas by modelling and (dynamic) pilot scale experiments.

The pilot scale set-up “GanyMeth” (that originally was planned to be used for the experimental part) unfortunately was delivered late in 2016; moreover, recent control of the delivered tubing showed severe problems with respect to the welding quality which raises questions for the plant safety. At the moment replacement of all questionable tubing is ongoing. Although the erection of the set-up is funded by another project, the recent issues made it impossible to conduct reactive experiments before end of the project time. Instead, a synergy with another project (“Direct methanation of biogas”, DMB) was used. Within the DMB project, the TRL 5 plant Cosyma was connected to a biogas plant in Zürich. After achieving the goals of the DMB project (1000h operation), the operation of the installation was continued to conduct optimisation experiments. These experiments (combined with characterization of catalyst samples) focused especially on the addition of water, which has a significant influence on coke formation and the yield in the main reactor and the effort (CAPEX and OPEX) in the upgrading step of the process.

Further, the efforts were increased to model and optimise in detail the complete process chain of biogas based power-to-gas. For this, the main units (reactors, membranes) were represented by rate-based models, while other process units were calculated with thermodynamic and short-cut models. The detail description of six different process concepts allowed also detailed cost calculations. The results obtained in this thermo-economic analysis can also be applied for the optimization of all other Power-to-Methane process chains.

2.2. Main Achievements

a) *Hydrogen addition to hydrothermal gasification/methanation*

Catalytic Hydrothermal Methanation (CHM) – experimental validation

For this study, we used the existing hydrothermal gasification unit KONTI-C and modified it for hydrogen co-feeding (Fig. 10). The model solution consisted of a mixture of 10 wt.% glycerol in de-ionized water. The feed mass flow rate was manually adjusted to 1.00 ± 0.02 kg/h and measured online using a Coriolis mass flow meter. The pressure of the test rig was adjusted to 28 or 26 MPa. Hydrogen from a cylinder (Messer Schweiz AG 4.5) was compressed to pressures of ~2-3 MPa above that pressure by a pneumatically controlled compressor (SITEC AG, Switzerland) and injected continuously upstream of the salt separator. The hydrogen flow rate was controlled by a mass flow controller.

The lower part of the catalytic reactor was filled with 713 g of a dry sulfur adsorbing material (Katalco 32-5, Johnson-Matthey; up to ca. 60 cm height), followed by a layer of dry 5 wt.% Ru/C catalyst (BASF; 493 g). Katalco 32-5 was filled in the reactor to adjust the height of the catalyst bed and to be comparable with other experiments having been conducted in the test rig KONTI-C.

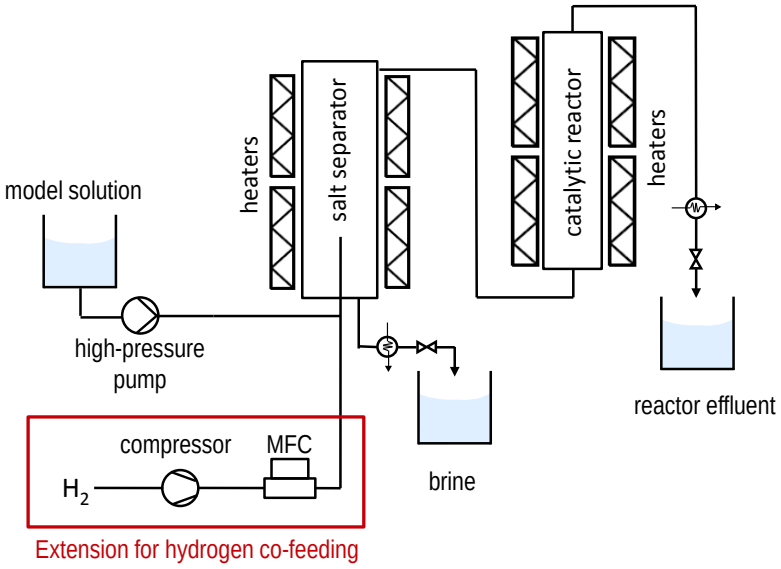

Fig. 10 Simplified representation of the hydrothermal gasification test rig KONTI-C including the possibility of hydrogen co-feeding with a mass flow controller (MFC). Some valves, pressure sensors, and thermocouples are omitted for clarity.

We selected seven different operating conditions including two different pressures and three different hydrogen flow rates (Table 3). The feed flow rate and the nominal reactor temperature were kept constant. Upon hydrogen addition the temperature profile in the reactor changed drastically (Figure 11). An increase of 75 K was measured at the beginning of the catalytic bed, indicating a vigorous reaction involving H_2. The peak temperature decreased along the catalytic bed and reached the same value as without H_2 at the end of the bed.

Tab. 3 Set points for the hydrothermal gasification experiments with 10 wt.% glycerol in water conducted in the test rig KONTI-C (T_SA: Temperature at the outlet of the salt separator, T_R: Temperature along the catalyst bed when operated on pure water; STP: 25 °C, 0.1 MPa)

Exp.	p / MPa	λ (H_2)	$\dot{V}_{STP}$ (H_2) / L/min	$\dot{m}^{H_2} / \dot{m}^{Glycerol}$	T_SA / °C	T_R / °C	$\dot{m}^{Feed}$ / kg/h
A	28	0	0	0	420	400	1.00
BA	28	0	0	0	420	400	1.00
BB	28	0.6	1.2	0.07	420	400	1.00
BC	28	1	2.0	0.11	420	400	1.00
CA	26	0	0	0	420	400	1.00
CB	26	0.6	1.2	0.07	420	400	1.00
CC	26	1	2.0	0.11	420	400	1.00

The gas composition shifted towards more methane and less CO_2, as expected, upon addition of hydrogen (Figure 12). The highest methane concentration of 86 vol% was reached when hydrogen was added stoichiometrically (λ = 1) at 28 MPa. Without added hydrogen, the methane concentration was 56 vol%. Decreasing the pressure to 26 MPa had almost no influence on the gas composition (not shown). This measured gas composition at 28 MPa comes close to the composition calculated for equilibrium conditions (see next section). This equilibrium limitation means that a further increase in methane concentration is only possible by reducing the temperature, which is undesired for kinetic reasons. A separation and recycling of the remaining H_2 would be the preferred method.

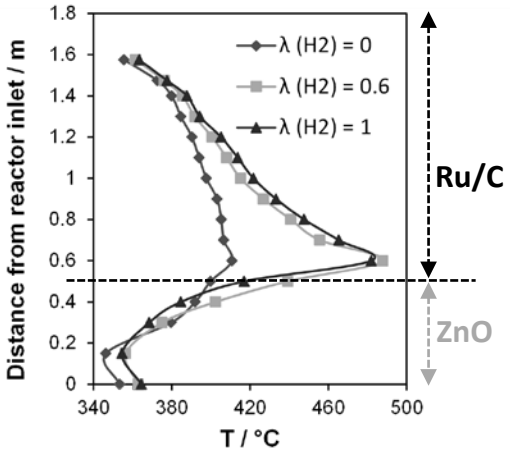

Fig. 11 Temperature profiles in the fixed-bed reactor during hydrothermal gasification of 10 wt.% glycerol in water for different hydrogen-to-glycerol ratios (Exp. BA, BB and BC, Tab. 3.1) at a total pressure of 28 MPa. The solid lines are guides to the eye

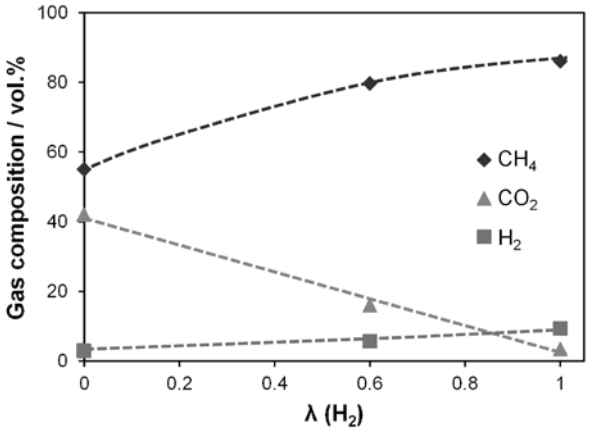

Fig. 12 Gas composition during the experiments at 28 MPa pressure (Exp. BA, BB and BC, Tab. 3.1) as a function of the parameter λ which defines the stoichiometric dosage of hydrogen according to Eq. (1). The broken lines are guides to the eye

Full catalytic activity was maintained during and after the hydrogen co-feeding experiments, verified by comparing the performance of a run with a 10 wt.% glycerol in water feed after co-feeding hydrogen, for which the product distribution was very close to the experiments before hydrogen co-feeding (Reimer et al., 2017).

Catalytic Hydrothermal Methanation (CHM) – process simulations

We have set up a flowsheet simulation of our continuous test rig using the software ASPEN plus V 8.0 (Fig. 13).

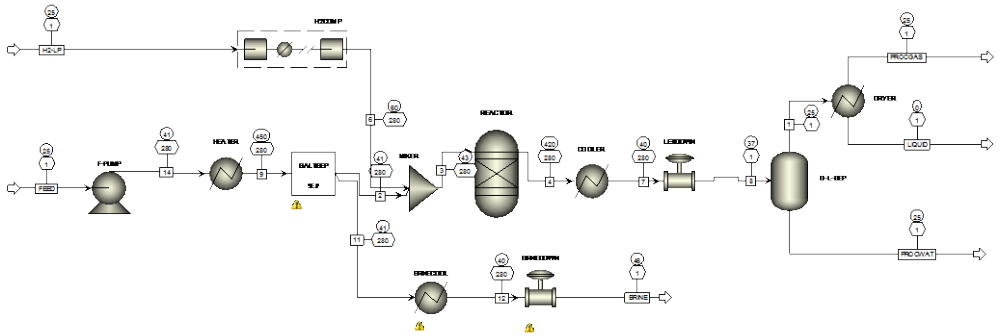

Fig. 13 Flowsheet for the simulated CHM process.

A water-glycerol mixture is pumped at 28 MPa and at a flow rate of 1 kg/h, corresponding to the capacity of our test rig “KONTI-C”. It is then heated to 450°C and mixed with a hydrogen stream pressurized to 28 MPa. Prior to mixing, salts optionally added to the feed mixture can be removed from the process stream in PSI’s patented salt separator. This brine is cooled and depressurized and collected for further use e.g. as fertilizer. The main process stream with the water-glycerol-H_2 mixture is reacted over the catalytic fixed-bed reactor containing the carbon-supported ruthenium catalyst at 420°C and 28 MPa. After cooling and depressurizing the liquid water phase and the gas phase are separated. The gas phase is cooled in a chiller to remove water vapor.

A series of simulations was run as indicated in Table 4.

Tab. 4 Process conditions used in the flowsheet simulation of the CHM process

w_Glyc kg/kg	m*_Feed kg/h	Brine frac kg/kg	V*_H_2 NL/h	λ_H_2 mol/mol	p MPa	T_reac °C
0.2	1	0.15	210	0.86	28	420
0.2	1	0	0	0.00	28	420
0.2	1	0	49	0.20	28	420
0.2	1	0	98	0.40	28	420
0.2	1	0	146	0.60	28	420
0.2	1	0	195	0.80	28	420
0.2	1	0	244	1.00	28	420
0.2	1	0	268	1.10	28	420
0.2	1	0	292	1.20	28	420
0.2	1	0	219	0.90	28	420
0.2	1	0	317	1.30	28	420

The concentration of the glycerol was fixed to 20 wt%, which is a typical value for the CHM process. In the first simulation, a brine stream corresponding to 15% of the total feed stream was withdrawn before the catalytic reactor. In all other simulations, no brine stream was withdrawn. Hydrogen was added in varying amounts to yield the lambda values indicated in Table 3.2. Here, lambda is defined as:

$$\lambda = \frac{\dot{n}_{H2}}{5\,\dot{n}_{glycerol}} \qquad (1)$$

This value describes the effective amount of hydrogen fed to the amount needed for stoichiometric conversion of the glycerol to methane and water according to:

$$C_3H_8O_3 + 5\ H_2 = 3\ CH_4 + 3\ H_2O$$

In the flowsheet simulation the equilibrium composition of the process stream leaving the catalytic reactor is then calculated taking the non-ideal behavior of the water-glycerol-H_2/CO_2/CH_4 mixture into account (Peng-Robinson equation of state). The resulting dry gas composition is shown in Fig. 14.

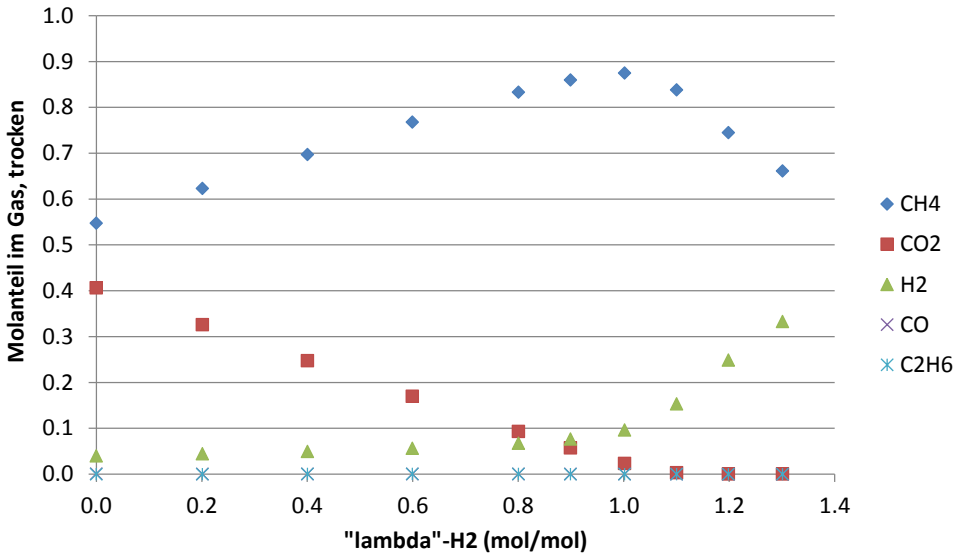

Fig. 14 Calculated dry gas compositions for the CHM process with varying amounts of added H_2 at 420°C and 28 MPa.

The gas composition for λ = 0 corresponds to the “classical” CHM process, i.e. without extra H_2 added. Upon addition of H_2 the methane concentration increases while the CO_2 concentration decreases, and the H_2 concentration remains relatively stable below 10 vol%. At λ = 1 a maximum in the methane concentration is reached. For higher λ values the CO_2 concentration decreases further but the methane concentration decreases as well, while the hydrogen concentration increases.

For $\lambda > 1$ it is thus possible to reduce the CO_2 content to almost zero but at the cost of "diluting" the product gas with the remaining excess H_2. Both carbon monoxide and ethane are not formed at these conditions. The highest methane concentration is thus reached for $\lambda = 1$, but it does not exceed 88 vol% because of the remaining H_2 and CO_2 at these conditions. A higher methane concentration could be reached by operating at lower temperatures, but this would affect the kinetics and thus the space velocity needed to approach the calculated equilibrium composition.

From the simulations a constant value of 15.3 MJ/kg was obtained for compressing the H_2 from ambient pressure to 28 MPa. A two-stage isentropic compression was assumed. For $\lambda(H_2) = 1$ the mass ratio of added H_2 to glycerol was 0.11. Thus ca. 1.7 MJ of external energy need to be supplied per kg of glycerol processed. For other feedstocks the amount of H_2 supplied corresponding to a $\lambda(H_2)$ value of one will vary depending on the H/C and O/C ratio of the feedstock.

Catalytic Hydrothermal Methanation (CHM) – dual source process heater

The overall idea of WP 2 is to integrate as efficiently as possible peak electric power that cannot be used instantly into the methanation or the hydrothermal gasification process. One way to reach this goal is to use the electric power to generate H_2 by electrolysis and to feed the pressurized H_2 into the catalytic processes. This first approach was described in the previous sections. Another approach, proposed here for the hydrothermal gasification (HTG) process only, is to use the electric power to heat the process directly. Since the HTG process must also operate when no peak electric power is available, a gas burner is used as a second energy source. Ideally, one and the same process heater can be operated on both energy sources, minimizing the investment cost. In Fig. 15 a schematic layout of such a dual source process heater is shown.

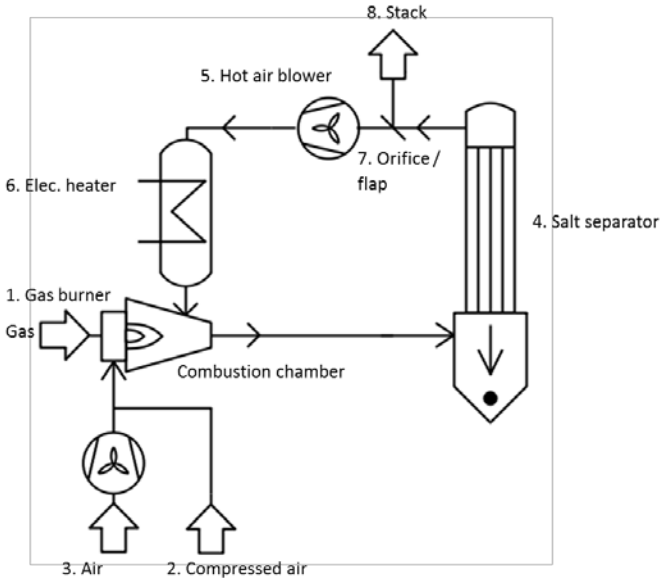

Fig. 15 Conceptual design for a dual process heater operated alternatively on a methane-rich gas and electricity. The hot gas circuit is used to heat the fluid inside the high pressure salt separator.

Its operation with a methane-rich gas is as follows:

- Ambient air (3) and gas are mixed and combusted in the burner (1) to produce an exit gas temperature of ca. 700°C.
- The pressure in the hot gas system can be adjusted to max. 0.5 bar using compressed air (2) and/or a hot air blower (5).
- The hot air flows countercurrent to the fluid in the salt separator (4), located inside a high pressure tube bundle.
- Recirculation of the hot air after the salt separator with a temperature of ca. 650°C by the hot air blower via the electric heater (6) into the combustion chamber.
- The gas burner (1) reheats the air to 700°C.
- Some hot air is vented to the atmosphere via a throttle orifice (7) and a stack (8).

Its operation with electric power is as follows:

- Cold air (2 or 3) is routed to the electric heater (6) via the gas burner (1), the salt separator (4) and the hot air blower (5).
- The pressure in the hot gas system can be adjusted to max. 0.5 bar using compressed air (2) and/or the hot air blower (5).
- The fresh air supply (2 or 3) is adjusted, as the hot air blower recirculates the air stream through the system.
- The electric heater (6) increases the temperature of the hot air up to the desired value.
- Some hot air is vented to the atmosphere via a throttle orifice (7) and a stack (8).

Such a system could be switched fast from gas to electric operation and back again. It can use both low and high calorific gases and reaches a high efficiency due to the recirculation loop. When available, air preheated to max. 250°C could be used, further increasing the overall efficiency by reducing the consumption of gas or electricity. Gas burners are commonly used in industrial heating. Electric heating of gases to high temperatures is less common. Fig. 16 shows a commercial system that could be used for the HTG process.

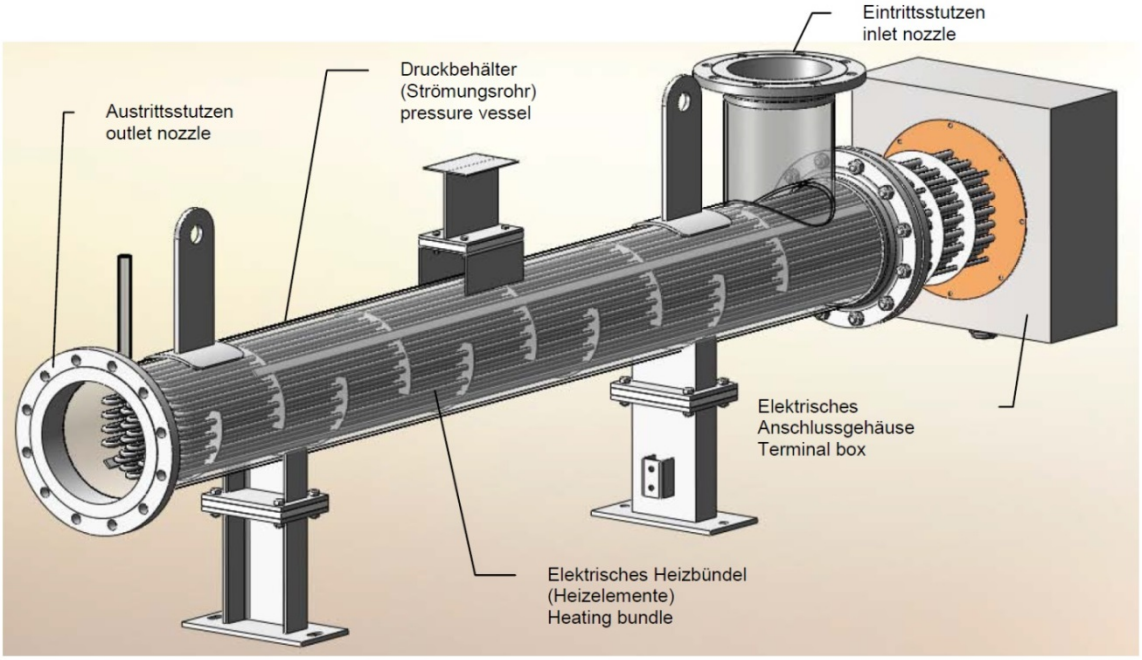

Fig. 16 Electric air heater Typ STR (OhmEx GmbH, Germany).

b) *Hydrogen-rich methanation of CO_2-containing gases*

Process modelling

In the modelling of CO_2-methnation processes, different processes were considered in the investigation of biogas upgrading. For this, the main units (reactors, membranes) were represented by rate-based models, while other process units were calculated with thermodynamic and short-cut models. The detail description of four different process concepts allowed also detailed cost calculations. Not only the fluidised bed technology was investigated, but also fixed bed technology in order to convert carbon dioxide into methane. As a result, four considered processes are listed in Table 5.

Tab. 5 Overview of the process models for biogas upgrading

Model description	Abbreviation
Biogas upgrade via bubbling fluidised bed (BFB) and fixed bed (FB)	BFB-FB
Biogas upgrade via two-stage FB technology	FB-FB
Biogas upgrade via BFB and H_2-membrane	BFB-Mem
Biogas upgrade via FB and H_2-membrane	FB-Mem

The corresponding flowsheets of the models are illustrated in Figures 17 and Figure 18. The procedure allows the direct comparison of fixed bed and fluidized bed technology. The approach of the process evaluation was as follows: First an optimization of the operational conditions via difference-in-cost method was applied. This means that the changing costs due to a specific combination of operation conditions (and according reactor designs) were compared to a base case. Secondly, a detailed economic analysis of the optimized process was conducted, which allowed the comparison with the other optimized processes.

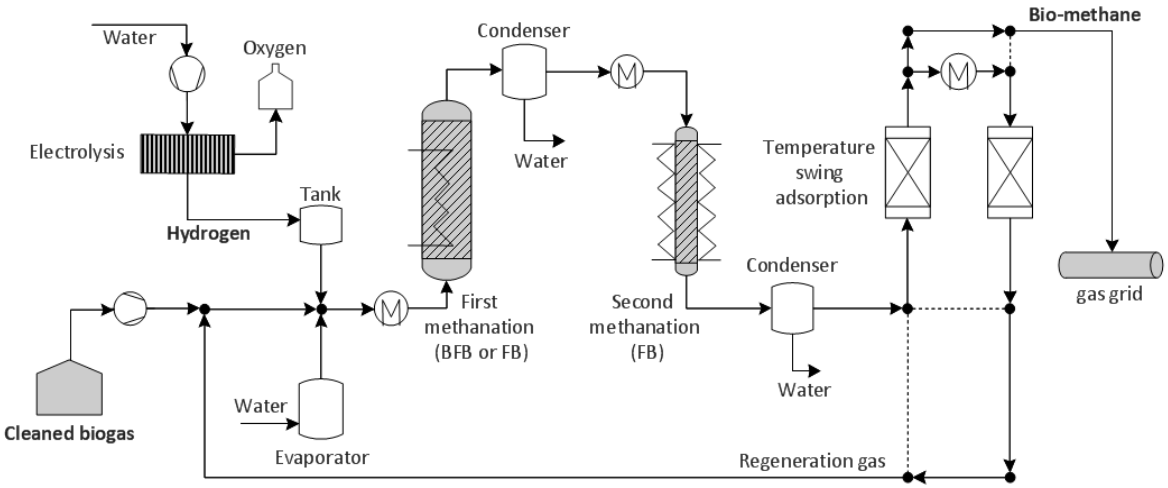

Fig. 17 Flowsheet of the upgrade process of biogas via two-stage methanation according to the models BFB-FB and FB-FB

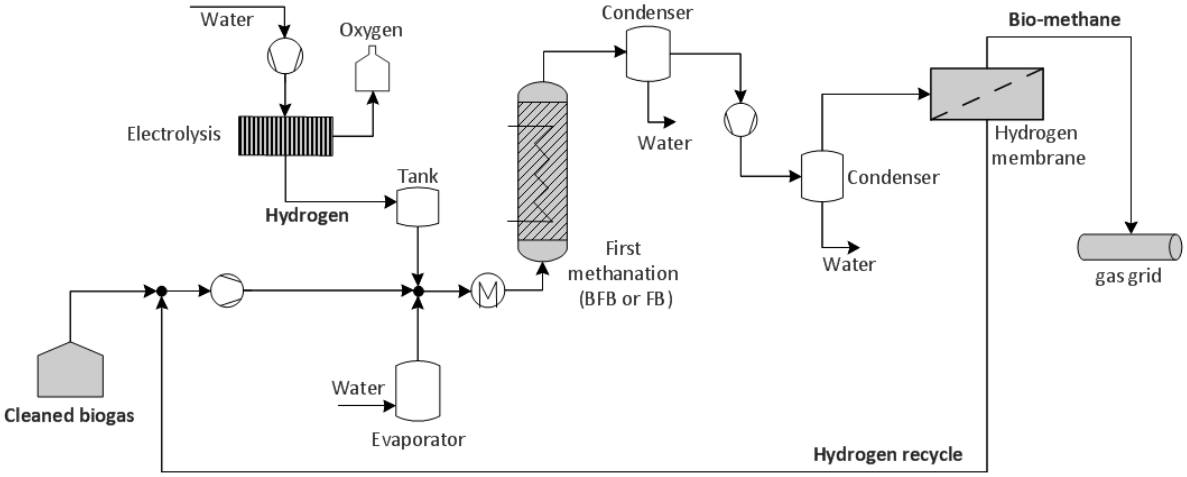

Fig. 18 Flowsheet of the upgrade process of biogas via methanation and hydrogen separation with a membrane according to the models BFB-Mem and FB-Mem

Reactor models

Isothermal bubbling fluidised bed reactor. The internally cooled fluidised bed reactor is modelled according to the pseudo-homogeneous two phase approach of Kopyscinski et al. [18] where hydrodynamic correlations for freely bubbling fluidized beds are applied.

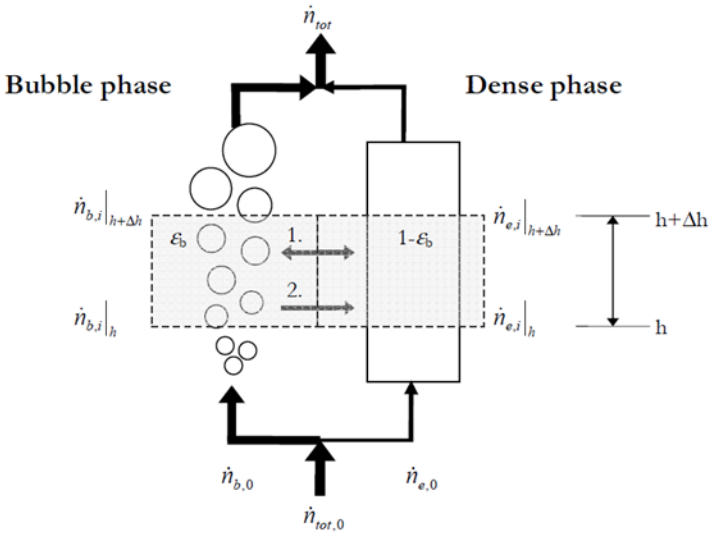

Fig. 19 Two phase model used for the bubbling fluidised bed model

According to Fig. 19, the total inlet gas flow $\dot{n}_{tot,0}$ is divided into the bubble $\dot{n}_{b,0}$ and the dense phase $\dot{n}_{e,0}$ gas flow, corresponding to the volumetric fraction of the bubble phase ε_b and of the dense phase $\varepsilon_e = 1 - \varepsilon_b$. The volumetric fraction of the bubble phase is determined by the following equation from Hilligart et al. [9] via superficial velocities u and bubble diameters d_b derived from bubble size correlations:

$$u_b = \psi\left(u - u_{mf}\right) + 0.711\,\upsilon\sqrt{g\,d_b} \tag{3}$$

$$\varepsilon_b = \frac{\psi\left(u - u_{mf}\right)}{u_b} \tag{4}$$

The parameters ψ and υ consider the different types of Geldart particles and depend on reactor height and diameter. The molar balances for the bubble and dense phase are shown in Equation (5) and (6), respectively.

$$0 = -\frac{d\dot{n}_{b,i}}{dh} - K_{G,i} \cdot a \cdot A_{cross} \cdot \left(c_{b,i} - c_{e,i}\right) - \dot{N}_{vc} \cdot x_{b,i} \tag{5}$$

$$0 = -\frac{d\dot{n}_{e,i}}{dh} + K_{G,i} \cdot a \cdot A_{cross} \cdot \left(c_{b,i} - c_{e,i}\right) + \dot{N}_{vc} \cdot x_{b,i} + \left(1 - \varepsilon_b\right) \cdot \left(1 - \varepsilon_{mf}\right) \cdot \rho_P \cdot A_{cross} \cdot R_i \tag{6}$$

Here, $(1-\varepsilon_b)$ represents the volume fraction of the dense phase, $(1-\varepsilon_{mf})$ express the volume fraction of the particles assuming minimal fluidisation conditions in the dense phase and $R_i = \sum \nu_{im} r_m$ describes the overall reaction, where m represents the WGS and methanation reactions.

Between the two phases, mass transfer occurs due to concentration differences but also due to the mole reducing reaction. The interphase mass transfer is described as the sum of the two phenomena, see Equation (7).

$$\dot{N}_{vc} = \frac{\dot{n}_{vc}}{dh} = \sum_i K_{G,i} \cdot a \cdot A \cdot \left(c_{b,i} - c_{e,i}\right) + \left(1-\varepsilon_b\right) \cdot \left(1-\varepsilon_{mf}\right) \cdot \rho_P \cdot A \cdot \sum_i R_i \tag{7}$$

The following assumptions for the differential equations were made: steady state conditions and ideal gas behaviour are assumed with no reaction in the bubble phase. Laminar boundary layers around the catalyst particles as well as pore diffusion are neglected; hence gas concentrations in the dense phase and on the catalyst particles are equal. Radial gas concentrations differences are neglected. Two main aspects influence the performance of the reactor: the reaction kinetics and the hydrodynamics caused by the bubbles inside of the reactor. For the kinetics, a Langmuir-Hinshelwood approach was implemented with rate equations for the water gas shift reaction:

$$r_{WGS}^{BFB} = \frac{k_{WGS}\left(K_\alpha p_{CO} p_{H_2O} - \left(\frac{p_{CO_2} p_{H_2}}{K_{eq,WGS}}\right)\right)}{p_{H_2}^{0.5}\left(1+K_C p_{CO}^d p_{H_2}^e + K_{OH}\, p_{H_2O}\, p_{H_2}^{-0.5}\right)^2} \tag{8}$$

and for the methanation reaction:

$$r_{Meth}^{BFB} = \frac{k_{Meth} K_C\, p_{CO}^a\, p_{H_2}^b \left(1-\left(\frac{p_{CH_4} p_{H_2O}}{K_{eq,meth}\, p_{CO}\, p_{H_2}^3}\right)\right)^c}{\left(1+K_C p_{CO}^d p_{H_2}^e + K_{OH} p_{H_2O} p_{H_2}^{-0.5}\right)^2} \tag{9}$$

Rate and adsorption constants are based on the Arrhenius and Van't Hoff approach:

$$k_i = k_{i,T_{ref}} \exp\left(\frac{E_{A,i}}{R T_{ref}}\left(1 - \frac{T_{ref}}{T}\right)\right) \quad , i = WGS, Meth \tag{10}$$

$$K_j = K_{j,T_{ref}} \exp\left(\frac{\Delta H_j}{R T_{ref}}\left(1 - \frac{T_{ref}}{T}\right)\right) \quad , j = \alpha, C, OH \ldots \tag{11}$$

The values of the kinetic parameters are given in Table 6 [1].

Tab. 6 Kinetic and adsorption constants of the methanation and water-gas-shift rate expressions for the bubbling fluidized bed methanation [1].

Parameter	Unit	Value
$k_{WGS,ref}^{BFB}$	-	8.40
$k_{Meth,ref}^{BFB}$	-	1.08
$E_{A,WGS}^{BFB}$	kJ/mol	155.7
$E_{A,Meth}^{BFB}$	kJ/mol	63.1
$K_{\alpha,ref}$	bar^{-2}	0.36
$K_{C,ref}$	$bar^{-1.5}$	2.53
$K_{OH,ref}$	$bar^{-0.5}$	0.67
ΔH_{α}	kJ/mol	-1.7
ΔH_{C}	kJ/mol	-50.7
ΔH_{OH}	kJ/mol	-87.5
A	-	0.5
B	-	1
C	-	1
D	-	0.5
E	-	0.5
T_{ref}	K	598.15

The hydrodynamics of the reactor are expressed through bubble size correlations, with which bubble rise velocities and the bubble holdup ε_b are determined in a next step. This procedure allows the determination of the total surface area of the bubbles and then the interphase mass transport from the bubble into the dense phase. Then, the kinetic expressions are applied, which result in new molar flows of the components due to the reactions in the dense phase at a specific reactor height.

Different bubble size correlations for fluidised beds exist in the literature [10] - [11], but only at non-reactive conditions and without heat exchanger internals. Another study has shown that bubble growth is inhibited by the presence of internals [12], therefore the bubble size correlation with the smallest overall bubble size was chosen, as given by Werther [10]:

$$d_B = 0.835\left(1 + 0.272\,(u - u_{mf})\right)^{1/3}(1 + 0.0684\,h)^{1.21} \quad (12)$$

Since the bubble diameter influences the gas composition in the dense phase via the mass transfer area and therefore the reaction performance, a precise correlation is essential for the accuracy of the model.

Fixed bed reactor. The fixed bed (FB) methanation model is also based on kinetic expressions and considers the same chemical equations (1) and (2) as the bubbling fluidized bed (BFB) model. The shell-side cooled reactor includes internal tubes with an inner diameter of 2.5cm each, which contain the catalyst. The description of the applied pseudo-homogeneous first order

model can be found from [2]. Steady state conditions and ideal gas behaviour are assumed again with no radial concentration changes.

The applied axial molar balance and the energy balance for the fixed bed reactor are given by:

$$\frac{d\dot{n}_i}{dz} = \sum_m \nu_{im} r_m \cdot A_{cross} \cdot \rho_{cat} \tag{13}$$

$$G \cdot c_p \cdot \frac{dT}{dz} = \sum_j r_j \cdot \Delta H_{\mathrm{Re}ac,m} \cdot \rho_{cat} + \frac{4 \cdot U}{d_{tube}} \cdot \left(T_{wall} - T\right) \tag{14}$$

The overall thermal transmittance U is calculated at each step based on the actual gas composition according to the correlation for a particle bed for spherical particles of 1.8 mm diameter [23]:

$$\mathrm{Nu} = 0.223 \cdot \mathrm{Rep}\,0.6109 \cdot \mathrm{Pr}\,0.333 \tag{15}$$

And the corresponding expressions for the Nusselt, Reynolds and Prandtl numbers:

$$Nu = \frac{\alpha_{\mathrm{int}ernal} \cdot d_p}{\lambda_{Fluid}} \tag{16}$$

$$\mathrm{Pr} = \frac{c_p \cdot \eta}{\lambda_{Fluid}} \tag{17}$$

$$\mathrm{Re}_p = \frac{G \cdot d_p}{\eta} \tag{18}$$

The main thermal resistance is assumed to be in the internal gas phase between the catalyst particle and the inner reactor wall, hence the thermal transmittance is expressed through $\frac{1}{\mathrm{U}} = \frac{1}{\alpha_{\mathrm{internal}}}$, where the thermal resistance in the wall and outside the tube is neglected.

Two different sets of kinetic parameters were applied. For the main fixed bed reactor, kinetic data were taken from [2]. The catalyst described is thermally stable at high temperatures, but is less active at lower temperatures. The kinetics for the methanation reaction in Equation (14) are originally retrieved from the perspective of steam reforming [3], where the methanation reaction from CO to methane was defined as reversed reaction. Hence, the parameter $\mathrm{K_{Meth}}$ in equation (14) represents the equilibrium constant of steam reforming.

$$\mathrm{r}_{\mathrm{WGS}}^{\mathrm{FB}} = \frac{\mathrm{k_{WGS}}\left(\mathrm{p_{CO}p_{H_2O}} - \mathrm{p_{CO_2}p_{H_2}/K_{WGS}}\right)}{\mathrm{p_{H_2}}\left(1 + \mathrm{K_{CO}p_{CO}} + \mathrm{K_{H_2}p_{H_2}} + \mathrm{K_{CH_4}p_{CH_4}} + \mathrm{K_{H_2O}p_{H_2O}p_{H_2}^{-1}}\right)^2} \tag{19}$$

$$\mathrm{r}_{\mathrm{Meth}}^{\mathrm{FB}} = \frac{\mathrm{k_{Meth}}\left(\mathrm{p_{CO}p_{H_2}^3/K_{Meth}} - \mathrm{p_{CH_4}p_{H_2O}}\right)}{\mathrm{p_{H_2}^{2.5}}\left(1 + \mathrm{K_{CO}p_{CO}} + \mathrm{K_{H_2}p_{H_2}} + \mathrm{K_{CH_4}p_{CH_4}} + \mathrm{K_{H_2O}p_{H_2O}p_{H_2}^{-1}}\right)^2} \tag{20}$$

Rate and adsorption constants are determined analogously by the Arrhenius and Van't Hoff approach.

For the second stage fixed bed model, the same kinetic parameters as for the bubbling fluidised bed are applied (see Table 6). In comparison to the main reactor, the kinetic values applied here describe a more thermodynamically beneficial catalyst, because it is more active at lower temperatures. But the thermal stability is not as high as for the first catalyst bed. However, in the second stage fixed bed only medium temperatures are reached, because the reaction extent and therefore the reaction heat produced are low due to the small amount of remaining carbon dioxide in the inlet gas to the second stage reactor.

Membrane Model

For the membrane unit, a detailed model was implemented. Figure 20 shows a scheme of a membrane module with one fibre in co-current flow. The feed enters the module and flows outside along the fibre. Over the length of the module, gas components are permeating through the membrane wall into the fibre.

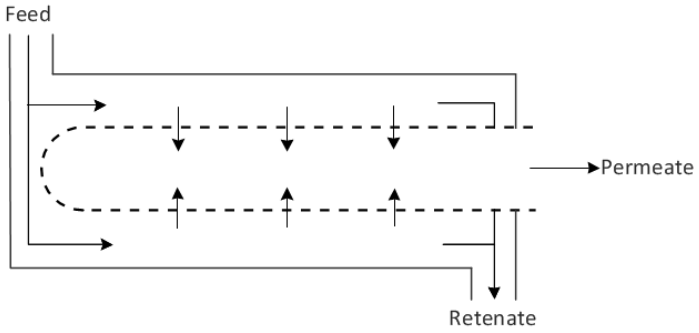

Fig.20 Simplified Scheme of a hollow-fibre module of a membrane

Ideal gas behavior and no pressure drop inside the fibre are assumed. The local permeation of gas through a non-porous membrane can be described by Fick's law [1]. It is assumed that the permeability of a pure component is not changing in a mixture or with varying pressure.

The model was implemented within a Matlab routine and executed inside a Matlab script, which describes the whole process. Values for the permeability constant are taken from [2] and [3]. The new model was compared with a short cut model, which is based on the expression of the selectivity for big pressure differences inside the membrane module [4]:

The result of the comparison between rigorous and short cut model is shown in Figure 20 and Figure 21, where the permeate flow and the retentate flow is illustrated over the membrane area for the different models. The pressure difference between permeate and retentate side was set to 27 bar. Permeability constants were chosen from [2].

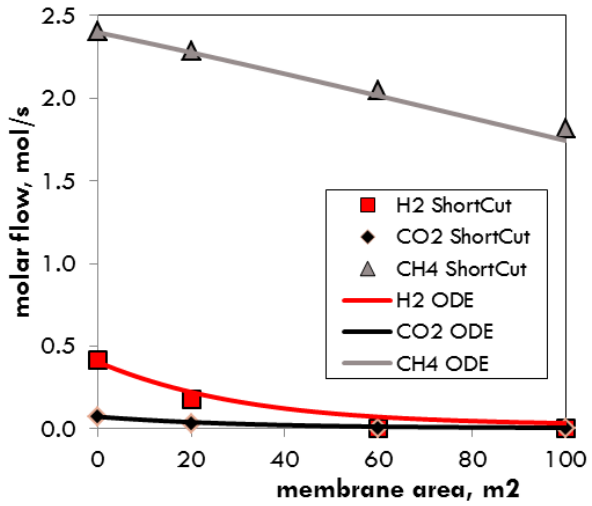

Fig. 21 Course of the molar flow of hydrogen, carbon dioxide and methane in the retentate over the membrane area for the short cut and the rigorous (ODE) model at a pressure difference of 27 bar

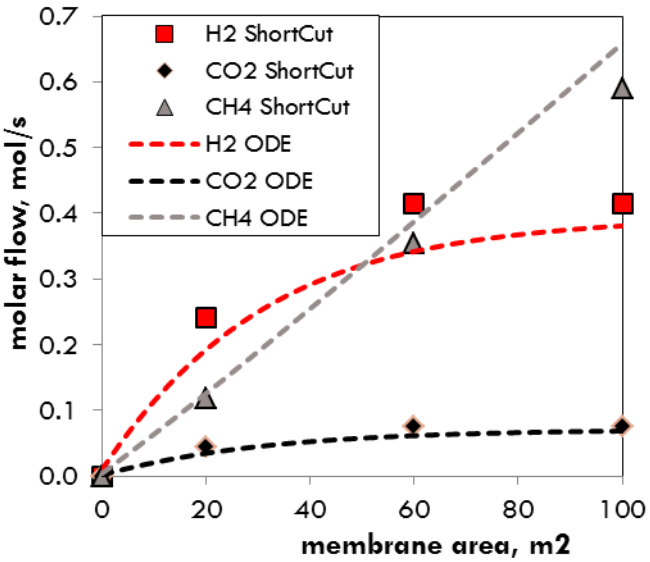

Fig. 21 Course of the molar flow of hydrogen, carbon dioxide and methane in the Permeate over the membrane area for the short cut and the rigorous (ODE) model at a pressure difference of 27 bar

It is apparent, that for big pressure differences between permeate and retentate side, the short cut model shows similar results in comparison to the rigorous model. However, small differences in the membrane model result in significant changes for the whole process. The aim of the membrane module is to lower the hydrogen amount in the retentate under 2 mole-%. The short cut model reaches this goal after 60m^2 of membrane area. The decline of hydrogen in the retentate calculated of the rigorous model is slightly weaker, but results in a significant higher membrane area needed for the separation target, which requires an area of 92 m^2.

If a bigger area is needed, it can be seen in Figure 21, that the permeate flow becomes more impure. The amount of methane and carbon dioxide in the permeate is increasing. For the whole process, this behavior results in a bigger recycle stream, which requires more compression power and causes higher electricity consumption. Because the rigorous model represents the real membrane behaviour better than the short cut model, the rigorous model should be used for the evaluation of the four processes mentioned above.

Results

With the improved membrane model, the four complete process chains were calculated in detail. Figure 22 shows as example the Sankey diagram (energy and mass flows) of one process concept. Due to optimization with continuous cost and efficiency functions for each process unit, pressures are chosen relative high, because this minimizes reactor dimensions. This procedure does not take into account technology jumps (e.g. choice of a different compressor type with different specific costs at a certain pressure difference), such that a pragmatic optimization considering more realistic technical options and commercially available units which finally may lead to slight deviating results.

While the four options lead to similar heat production and all are able to deliver injectable gas, the fluidized bed options lead to significantly lower reactor size (i.e. catalyst hold-up) and therefore costs.

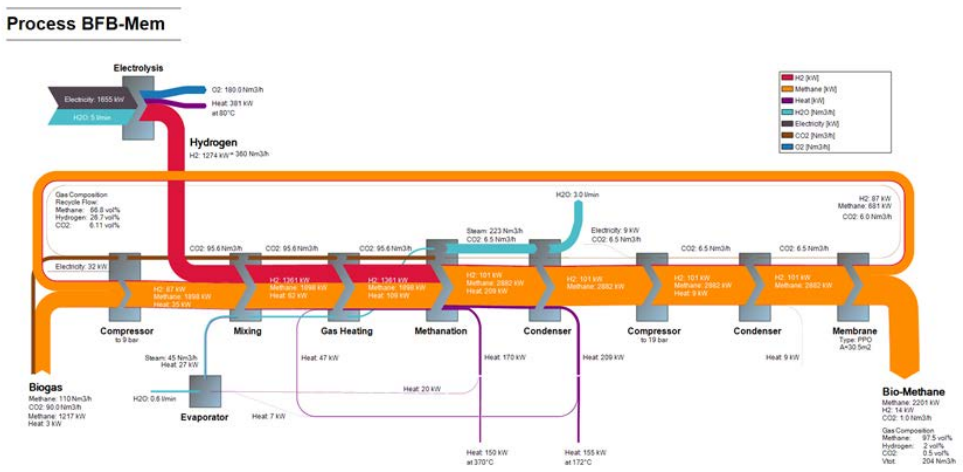

Fig. 22 Sankey diagram of modelled process chain

Table 7 Operational conditions and properties of optimal case for each process

	BFB-FB	FB-FB	BFB-Mem	FB-Mem
$P_{reactor}$ [bar]	12	14	12	25
p_{Mem} [bar]	-	-	28	28
$H_2/CO_{2,\ input}$	4.03	4.03	4.0	4.0
Membrane type	-	-	PPO	PPO
$T_{1.\ reactor}$ [°C]	375	354	380	373
$\dot{Q}_{excess}$ [kW]	241	223	249	245
$m_{Cat,tot}$ [kg]	88	211	67	193
$\dot{Q}_{el,tot}$ [kW]	1682	1695	1699	1702
Biomethane composition [mol%]:				
H_2	1.97	1.94	1.94	1.94
CO_2	0.16	0.15	0.44	0.48
CH_4	97.86	97.90	97.54	97.55

Experimental

A long-duration experiment was conducted within the project “Direct methanation of biogas”. For this, the set-up COSYMA including a bubbling fluidised bed reactor was transported to the biogas plant in Zurich-Werdhölzli. The chosen operation conditions for the long duration experiment were chosen based on simulations conducted within the RENERG^2 project. After achieving the goals of the DMB project (1000h operation), the operation of the installation was continued to conduct optimisation experiments. These experiments (combined with characterization of catalyst samples) focused especially on the addition of water, which has a significant influence on coke formation and the yield in the main reactor and the effort (CAPEX and OPEX) in the upgrading step of the process. Especially the tendency for coke formation could be tested within this set-up, because chemistry-related phenomena are more or less scale-independent.

Compared to the operation conditions during the long duration experiment, water/steam addition was first reduced by half for 45 h, and then stopped completely. This way the catalyst surface area is only covered by the biogas species and the water produced during the methanation reaction.

Figure 23 shows the molar fractions of the reaction product methane and the reactants CO_2 and hydrogen. During the first 1000h, activity slightly dropped, mainly due to slow catalyst poisoning by Sulphur breakthrough. After 1000h, the yield and in consequence the methane molar fraction increases again due to the lower addition of steam. A positive effect on the yield was expected because water competes with hydrogen in adsorbing on the catalyst surface, on the one hand, and it changes the thermodynamic equilibrium limitation to lower values, on the other hand.

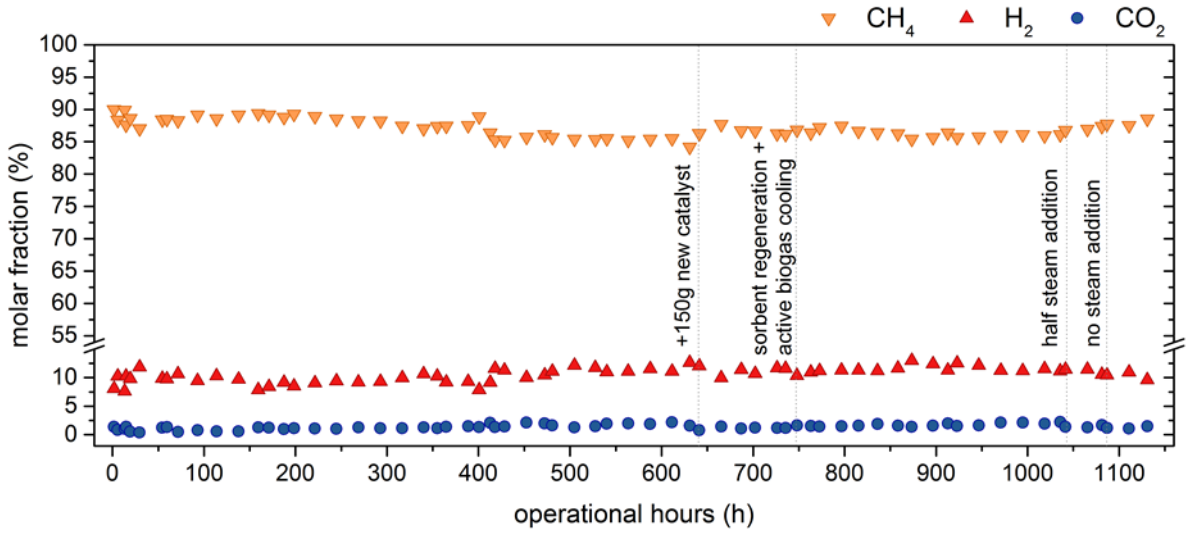

Fig. 23 Fractions of methane, hydrogen and CO_2 during the field test of COSYMA using real biogas at the biogasplant Zurich. Attention should be focused on the experimental results after 1000 where optimization of the water addition was conducted for the RENERG[2] project.

Lower steam addition, however bears the risk of carbon deposition due to the high amounts of carbon in the system. This was investigated by taking catalyst samples from the reactor (cooled material under nitrogen flow) and subsequent temperature programmed oxidation (TPO). During this analysis, carbon in the catalyst sample will burn and form CO_2 which is detected by e.g. a FTIR or a MS. Due to their different chemical stability of the carbon species, the temperature at which a carbon species burns varies. In Figure 24, the CO_2 evolution at 800°C (after 150 min) refers to graphite which is a component of the catalyst material and therefore visible even in the fresh material.

The CO_2 peaks rising at temperature between 150°C and 500°C are very typical for polymeric carbon deposition o the catalyst surface. While this peak is very strong for the catalyst samples from experiments with gasification derived producer gas (samples Cosyma 5 and 16), it is very weak for the samples from the biogas upgrading experiments. It can therefore be concluded that lowering the steam addition seems not to compromise the catalyst and process stability.

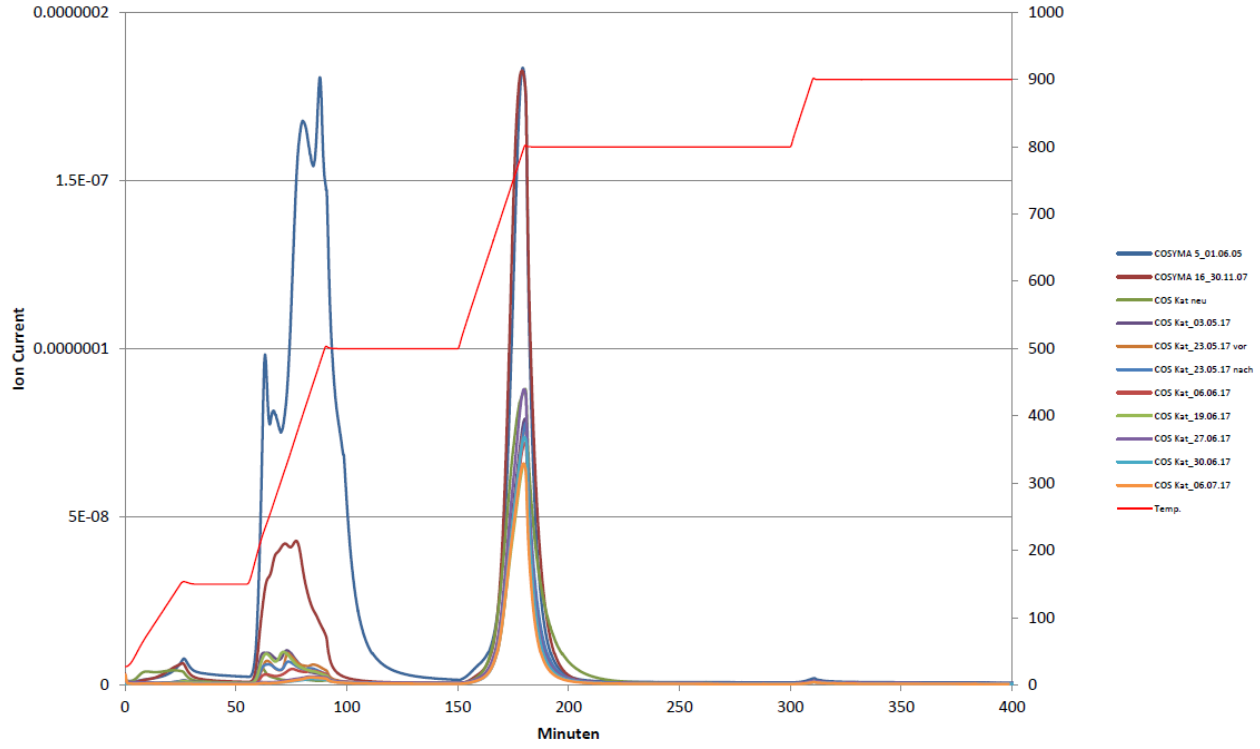

Fig. 24 Temperature programmed oxidation (TPO) of different catalyst samples from actual and previous (Cosyma 5, 16) experiments.

References

[1] S. L. Teske, “Integrating Rate Based Models into a Multi-Objective Process Design & Optimisation Framework using Surrogate Models,” vol. 6302, 2014.

[2] N. R. Parlikkad et al., “Modeling of fixed bed methanation reactor for syngas production: Operating window and performance characteristics,” Fuel, vol. 107, pp. 254–260, 2013.

[3] J. Xu and G. F. Froment, “Methane Steam Reforming , Methanation and Water-Gas Shift : 1 . Intrinsic Kinetics,” AIChE J., vol. 35, no. 1, pp. 88–96, 1989.

[7] Evonik, “Factsheet - SEPURAN® Noble - Membrantechnologie für Helium- und Wasserstoffaufbereitung,” 2016.

[8] J. Kopyscinski, T. J. Schildhauer, and S. M. A. Biollaz, “Methanation in a fluidized bed reactor with high initial CO partial pressure: Part II- Modeling and sensitivity study,” Chem. Eng. Sci., vol. 66, no. 8, pp. 1612–1621, 2011.

[9] K. Hilligardt and J. Werther, “Lokaler Blasengasholdup und Expansionsverhalten von Gas/Feststoff-Wirbelschichten,” Chem. Eng. Technol., vol. 57, no. 7, 1985.

[10] J. Werther, “Die Bedeutung der Blasenkoaleszenz fur die Auslegung von GaslFeststoff-Wirbelschichten,” Chemie Engenieur Tech., vol. 48, no. 4, p. 339, 1976.

[11] S. Mori and C. Y. Wen, “Estimation of bubble diameter in gaseous fluidized beds,” AIChE J., vol. 21, no. 1, pp. 109–115, 1975.

[12] S. Maurer et al., “Correlating bubble size and velocity distribution in bubbling fluidized bed based on X-ray tomography,” Chem. Eng. J., vol. 298, pp. 17–25, 2016.

2.3. Publications / patents

Reimer, J.; Müller, S.; De Boni, E.; Vogel, F. Hydrogen-enhanced catalytic hydrothermal gasification of biomass, *Biomass Conversion and Biorefinery*, published online, DOI 10.1007/s13399-017-0253-y.

Vogel, F. *Simulation of the addition of compressed H_2 to the hydrothermal gasification process*, internal report, Bioenergy and Catalysis Laboratory, Paul Scherrer Institut, Villigen PSI, September 6, 2017.

Witte J., Settino J., Biollaz S.M.A., Schildhauer T.J., *Direct Catalytic Methanation of Biogas – Part I: New Insights into Biomethane Production using Rate-Based Modelling and Detailed Process Analysis*, manuscript submitted

2.4. Industrial WP2 partner

- SFOE Swiss Federal Office of Energy
- Energie360° Energy supplier

3. HCNG field testing (WP3)

3.1. HCNG blending station

The overall target is the planning and realization of both an ad interims and a permanent HCNG refueling possibility on the basis of measurements and simulation works. Thereby the emphasis was put on HCNG-mixtures ranging from 0 to 30 vol-%. The following table shows exemplary HCNG-mixtures with corresponding volume, mass and energy fractions.

Tab. 8 Corresponding volume, mass and energy fractions of exemplary HCNG-mixtures

vol-%	mass-%	energy-%
2	0.23	0.55
10	1.25	2.95
25	3.65	8.33

The ad interims solution for HCNG refueling with low H_2 content was successfully taken into operation in the 3rd quarter of 2014 and decommissioned again roughly one year later. It allowed the refueling of three CNG vehicles tested as part of WP4.2 with a H_2 fraction of 2 vol-%.

Modelling and simulations of the CNG refueling process could be carried out as scheduled and were successfully validated with measurements taken on the CNG dispenser at Empa. Subsequently the model was extended to incorporate HCNG refueling which provided relevant support for the development of the permanent HCNG dispenser.

Commissioning of the permanent HCNG dispenser was planned for 2016 but had suffered a substantial delay. One of the project partners went into a lengthy reorganisation process in 2016 which resulted in the loss of project-relevant employees and know how. Also the procurement of the originally desired fuel system parts for the HCNG field test vehicle became uncertain and led to significant delays. Therefore, the successful commissioning of the permanent HCNG dispenser took place in August 2017. Since then the dispenser is in operation and allows the refueling of 0 to 30 vol-% of H_2 which lies in accordance with the proposed targets.

HCNG Field testing

The overall target is to demonstrate that CNG/hydrogen mixtures can be used as fuel in current vehicle powertrains on the basis of field test with different hydrogen blending ratios. The field testing with three standard vehicles, fueled with 2 vol-% hydrogen in CNG, was carried out as planned from 2014 to 2015, including chassis dyno tests to analyze the pollutant emission behavior. A paper on the effects of low hydrogen blending ratios (2 vol-%) in CNG is currently in progress and is expected to be submitted in the beginning of 2018.

The field testing of the specially prepared vehicle was planned to start in 2016 but due to the limited availability of hydrogen-compatible parts experienced significant delays. By the end of January 2017, all parts had finally been delivered. The vehicle's fuel system was rebuilt from February to June 2017 and was certified and approved for road traffic in July 2017. Since August 2017, the vehicle is now undergoing a field test a parcel delivery vehicle in the area of Dübendorf, fueled with a mixture of CNG and 25 vol.-% of hydrogen. The first months showed that the vehicle and the refueling are working properly with no negative side effects for the driver or the driving behavior, even though the engine control unit has not been modified an is still running in its factory setting for CNG.

Empa will carry out further detailed investigations and emission tests in the laboratory following the field test.

3.2. Main achievements

HCNG blending station

The following listing summarizes the main achievements throughout the complete project duration.

- Working ad interims solution for HCNG-refueling (meanwhile decommissioned again)
- Validated model for CNG refueling
- Various extended models for different HCNG refueling possibilities
- Working HCNG dispenser (0 – 30 vol-% H_2) controlled by self-developed algorithm
- HCNG refueling target pressures determined (taking into account molar fraction of H_2, initial car tank pressure, ambient temperature and compression heat release)
- Various HCNG refueling data from measurements and simulations collected

To enable real-world measurements on CNG vehicles with low H_2 admixture an ad interims H_2-dispenser was designed and built in collaboration with the company Apex AG and the project partner Endress+Hauser. Thereby a refueling concept was chosen which was not very user friendly but realizable in a short time. The pictures below show the main components of the self-developed H_2 dispenser (left) and the refueling equipment in general (right).

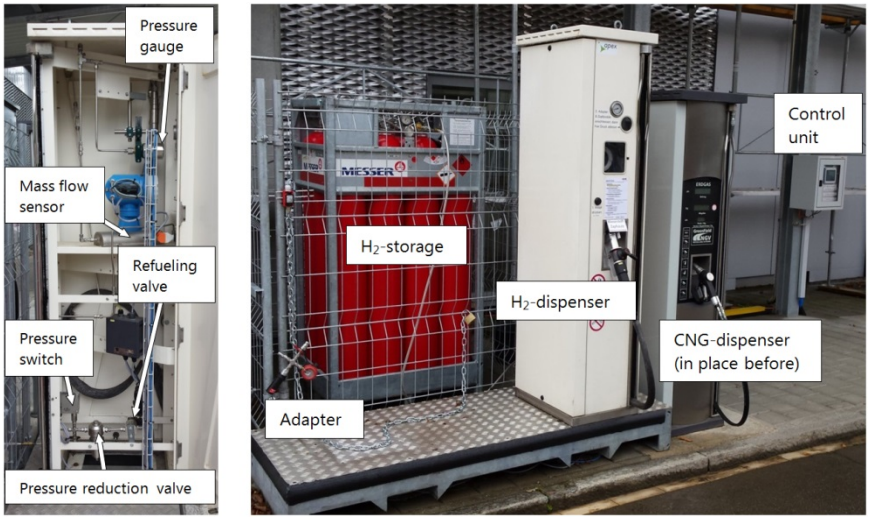

Fig. 25 Main components of self-developed H2 dispenser (left) and the refueling equipment in general (right).

For the user the process of refueling consisted mainly of five steps:

Fill fueling hose of the H_2-dispenser by pressing the black button above the nozzle
⇨ Enables the determination of initial tank pressure in step 3

1. Connect adapter and fueling nozzle of the H_2-dispenser
2. Read pressure from manometer at the dispenser and ambient temperature from gauge at the control unit to determine the amount of H_2 to be refueled from a table available on site
3. Enter determined amount in control unit and start H_2 refueling
4. After control unit stops H_2 refueling perform a conventional CNG-refueling at the CNG-dispenser

Next to designing a safe and reliably working H_2-dispensing unit and refueling process the main challenge lied in working out the table determining the amount of H_2 to refuel. This amount depends on the mass of CNG refueled subsequently at the conventional CNG-dispenser in step 5 which is not mass but pressure controlled. The CNG target pressure in turn is depended on the pressure after H_2-refueling, the ambient temperature and the temperature increase caused by compression heat release during H_2 and CNG refueling which is not readily determined. However, thanks to existing knowledge and measurements from tasks preceding this project the amount of H_2 to refuel could be estimated successfully using various rough calculations and the required degree of accuracy regarding mixing ratio was met.

The ad interims H_2-dispenser was decommissioned again in 2015.

Computer model for CNG-refueling

In parallel to the realization of the ad interims dispenser a 1D computer model for the conventional CNG refueling process was developed using the multi-physics software *AMESim*. The model particularly consists of the CNG station storage tanks, the dispenser, the car tanks and the system control as depicted in Figure 26.

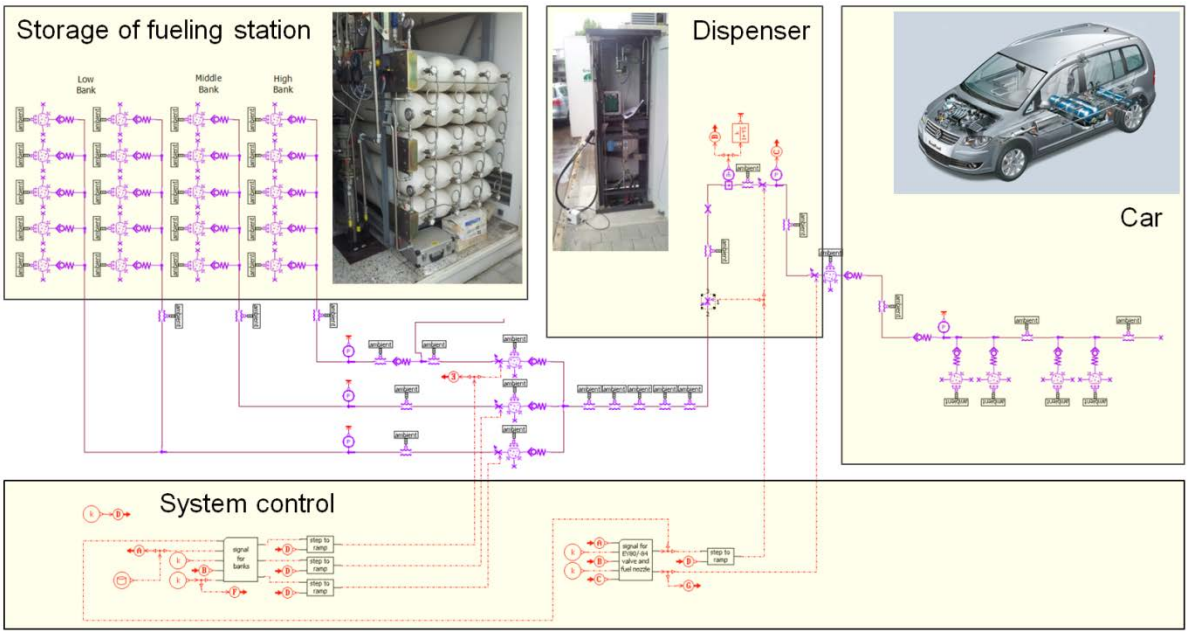

Fig. 26 AMESim simulation interface showing the main components of the CNG refueling model

The model allows the observation of pressure and temperature evolution in both storage and car tanks during a CNG refueling process. Whereas pressure losses in pipes and fittings as well as heat transfer through pipe and tank walls are accounted for, the one dimensional approach simplifies pressure and temperature in fixed volumes to be homogeneous at all times. Furthermore, CNG is approximated by CH_4 for which properties are available in the databank of *AMESim*. To incorporate real gas behavior the Peng Robinson equation of state was employed.

The system control was implemented in consultation with the project partner Atlas Copco. Various characteristics of a state-of-the-art CNG refueling controller such as determination of initial tank pressure, switching between storage tanks during refueling (cascade refueling) and the termination of the refueling process were implemented.

The simulation results were validated with measurements taken at the CNG-dispenser of Empa. As test vehicle a VW Touran EcoFuel CNG was used. After fine tuning the control parameters as well as all estimated coefficients determining pressure drop and heat transfer a good correlation between simulation and experiments was achieved.

The subsequent figures show data from three experiments and a simulation run of the pressure in the fueling hose as well as the mass flow of a CNG refueling at an ambient temperature of 8°C. The three experiments at almost completely equal conditions show, that the refueling process always incorporates some differences with respect to time, so that simulation results should have the same tendencies but not necessarily need to show precise temporal correlation compared to one experiment (Figure 27).

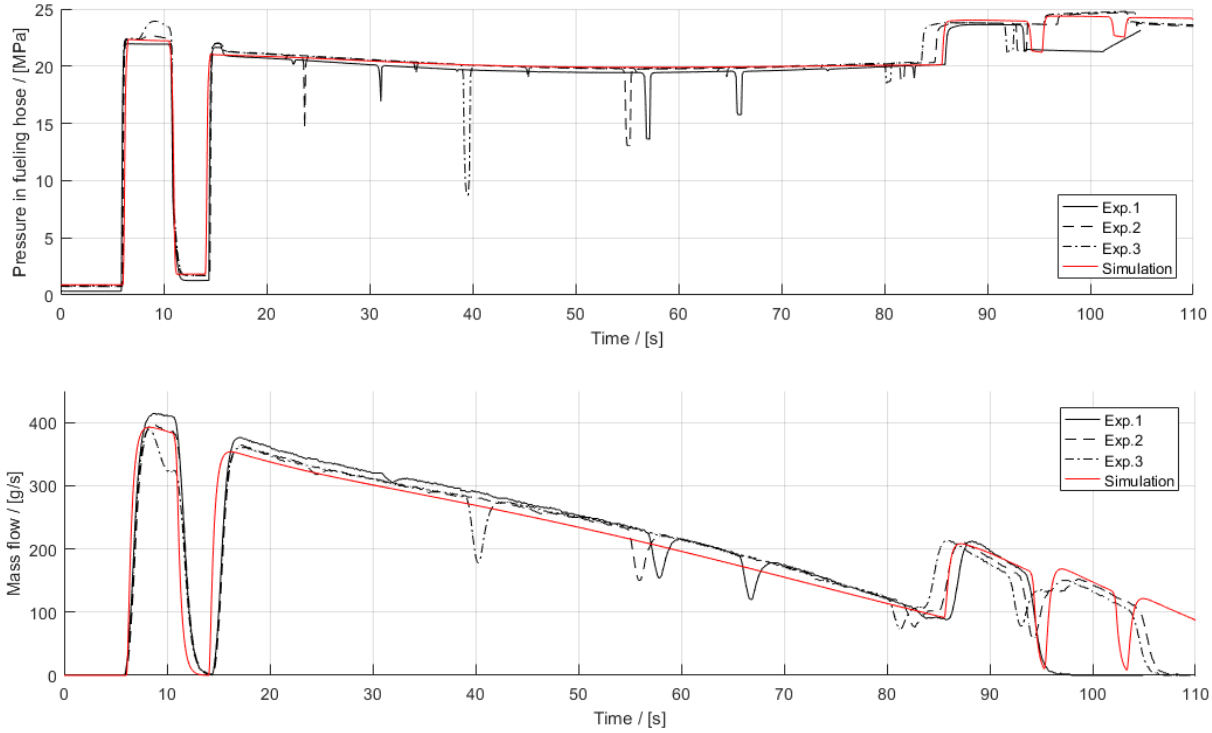

Fig. 27 Comparison of measurements and simulation regarding the pressure in the fueling hose (top) and mass flow (bottom) during CNG refueling

The figures display the pressure pulse in the beginning of the CNG refueling (6 s – 11 s) which allows the determination of the initial tank pressure. After around 14 s the actual refueling is started.

Subsequently the pressure in the fueling hose remains almost constant and the mass flow decreases continuously due to the decreasing pressure difference between storage tank and car tank. At around 85 s and 95 s refueling control switches to storage tanks with higher pressure (cascade refueling) leading to an increase in both fuel hose pressure and mass flow.

The dips in the curves are caused by pressure checks triggered by the system control. As these have no significant influence on pressure and temperature evolution during refueling they were omitted in the model.

While developing and validating the model the determination of the heat transfer within the car tank was identified as a task which needs very detailed attention going beyond the scope of this project. In particular regarding the heat transfer coefficient from the gas to the car tank wall no useful literature data could be found. Not least due to this reason a new project proposal was submitted to the SFOE for a more in-depth investigation of the temperature and heat transfer behavior within the car tank during refueling of gaseous fuels. The project is called 'eHF – efficient Hydrogen Fueling' and is scheduled to start in the 3rd quarter of 2017.

Model extension for HCNG-refueling

The validated model for the CNG refueling process forms the basis for the investigations of different HCNG refueling processes. To support the evaluation of refueling strategies for the permanent HCNG-dispenser (0 - 30 vol-% H_2) the CNG model was extended by various set-ups for H_2 addition. Particularly, online mixing of CNG and H_2 as well as intermittent and subsequent addition of H_2 was investigated. Furthermore, the set-ups were rated according to criteria such as functionality, system simplicity, cost of components etc.

For the HCNG-dispenser at Empa, however, the subsequent type refueling remained as the only option. Due to the decrease of volumetric energy density when adding H_2 to CNG it was decided to increase the nominal car tank pressure of the HCNG test vehicle from 20 MPa to 35 MPa. As a result, the HCNG mixture in the car tank can only be achieved by refueling CNG first and adding H_2 subsequently since the pressure in the CNG storage tanks cannot exceed 27 MPa.

In any case, subsequent-type refueling performs very well regarding system simplicity and cost aspects. However, as CNG is only available at 27 MPa in case of the Empa station, a complete HCNG-refueling with high initial tank pressure will not be possible as can be observed in the diagram showing the CNG target pressures later in this chapter. Also, manual cancellation during a refueling process will lead to undesired mixing ratios.

Among other things the extended model for the subsequent-type HCNG-refueling was used to analyze the gas temperature inside the car tank. The figure below shows the mass flow of CNG and H_2 as well as the resulting average temperatures within a specific car tank (in this figure it's tank no. 3) during subsequent refueling. As heat transfer through the car tank is not readily determinable, two different insulation scenarios where analyzed in this example. The blue curve depicts the result for a simulation run with low and the green with high heat transfer to the ambient.

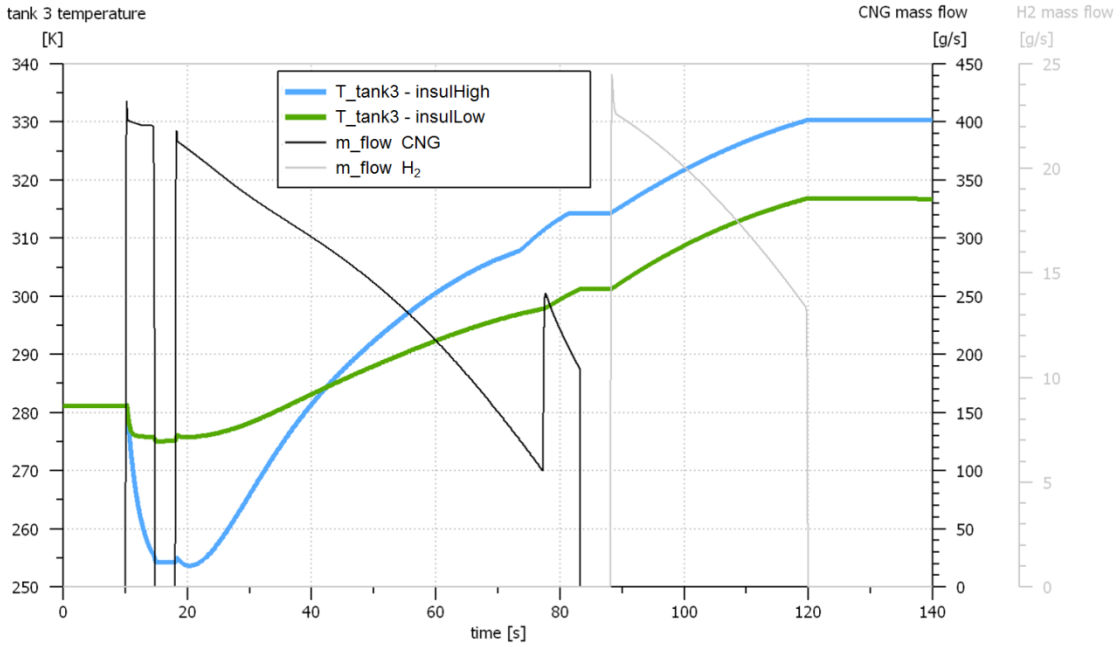

Fig. 28 Mass flow and temperature evolution for different heat transfer scenarios of a subsequent-type HCNG-refueling

On one hand knowing the gas temperature within the car tank is important to ensure that the normative temperature limit of 85°C for type IV tanks (as installed in the test vehicle) is not exceeded. With low heat transfer and higher ambient temperatures HCNG-refueling could lead to gas temperatures in the region of this limit. In such case the refueling time needs to be extended to allow more time for heat dissipation so that damage to the car tanks is prevented.

On the other hand the gas temperature needs to be known to determine the necessary storage tank pressures at the station. If gas temperature in the tank rises to high values the car needs to be filled to a pressure significantly higher than the nominal pressure of 35 MPa. If the station storage does not allow sufficiently high pressure levels – as is the case for the Empa station – the CNG refueling needs to be stopped early so that it is possible to refuel enough H_2. By doing so, the car tank will not be filled to full extent but the desired H_2 fraction can be achieved.

While looking into different HCNG refueling processes the question arose, if subsequent or intermittent refueling would cause the HCNG mixture to be inhomogeneous inside the car tank. For that reason very basic measurements using a gas analyzer were conducted to investigate the respective issue. The measurements showed that CNG and H_2 seem to mix well even when refueling subsequently, however, more in-depth analyses are necessary for conclusive statements. Also the fact that refueling lines of the car will be filled with mainly H_2 at the end of a subsequent HCNG-refueling was examined with basic investigations which showed that it doesn't seem to be an issue. Hereby detailed research would need to be conducted as well.

HCNG refueling dispenser

Based on the experiences gained from simulations and experiments in the first two years of the project the permanent HCNG-dispenser was designed at Empa and built by the project partner Atlas Copco. The main components of the HCNG dispenser are shown below.

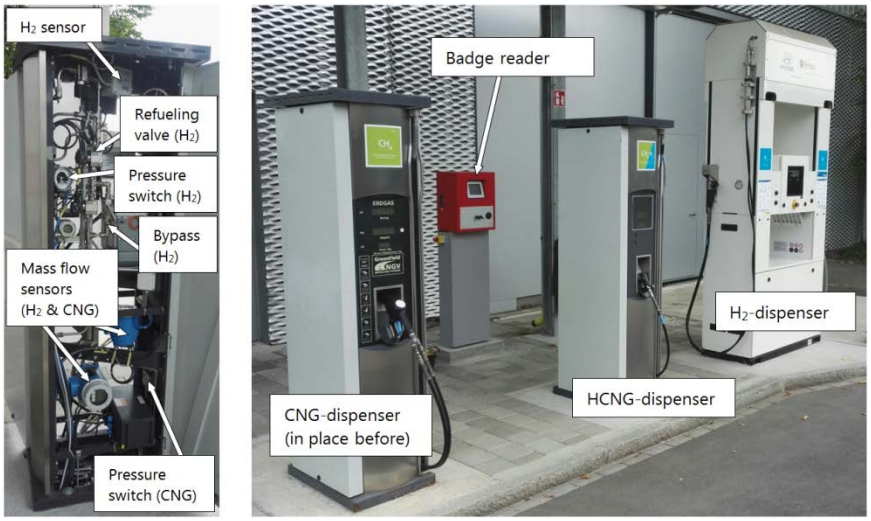

Fig. 29 Main components of the self-developed HCNG dispenser (left) and the refueling station at the move demonstration plant (right)

In contrast to the ad interims solution the permanent HCNG refueling dispenser allows HCNG mixtures from 0 to 30 vol-% and refueling is possible without compromising on convenience in comparison with a conventional CNG dispenser. The refueling process is governed by three controllers:

- SEKA (Atlas Copco) Controls first part of CNG refueling including cascade refueling
- Beckhoff SPS Controls second part of CNG refueling and has overall control
- Batch Controller Controls H_2-refueling

The complete refueling strategy and with that also the main logic for the HCNG refueling process was developed at Empa and is implemented in the Beckhoff SPS which has overall control of the refueling. It was programmed using the automation software TwinCAT from Beckhoff that is embedded in Microsoft Visual Studio. Following screenshots are intended to give an idea of the software interface (left) and the visualization tool (right) of the software.

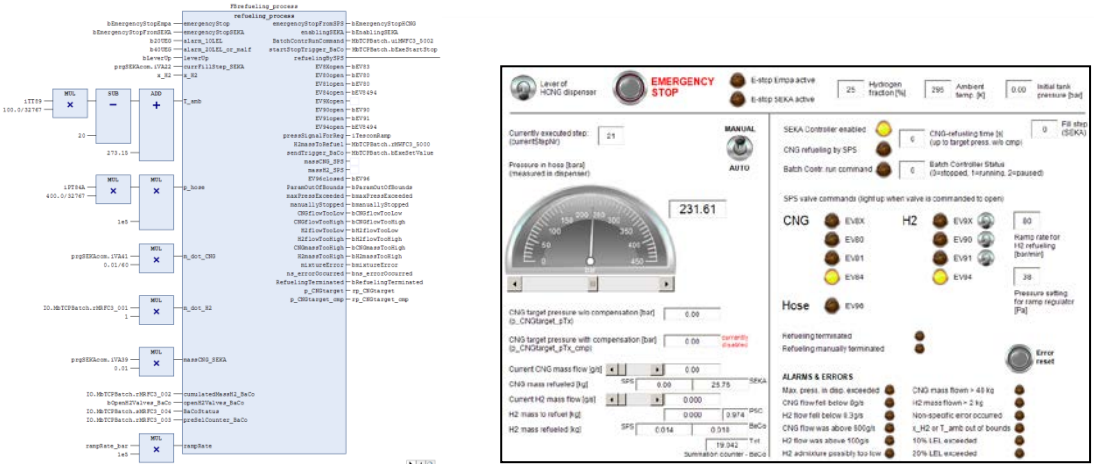

Fig. 30 TwinCAT programming interface (left) and visualization (right)

Target pressure determination

Since many relevant parameter are unknown to the HCNG dispenser control (car tank volume & insulation, number of car tanks, car tank pressure & temperature, etc), the data measured at the station site in combination with calculations and assumptions is used for governing the refueling process. As the CNG refueling part is pressure controlled, the determination of the CNG target pressure is of key importance for process control. The target pressure is influenced by the following parameters:

Tab. 9 Determination of parameter influencing CNG target pressure calculation

Influencing parameter	Determination of parameter
Initial car tank temperature	Ambient temperature measurement at station site
Initial car tank pressure	Pressure measurement in dispenser after 1st pressure pulse
H_2 fraction	Predefined through Beckhoff SPS
Final car tank temperature	Estimated by simulations and empirical formulas

The target pressure is set so that the energy content of the HCNG-mixture in the car tanks remains equal independent of the parameters listed above. This means that if the car tanks are completely filled, the energy content is always intended to be equal to the energy content of CNG at 20 MPa and 15°C. The H_2 fraction in the car tanks at the beginning of the refueling is not determined. Instead it is assumed that the mixture within the car tank corresponds to the mixture to be refueled. As it is planned to operate the test vehicle with the same mixture for several months this assumption is valid.

The figure below shows the CNG target pressure in dependence of the H_2 fraction. The dependency on initial car tank pressure is depicted exemplary for a value of 2 MPa (green) and 15 MPa (blue). Similarly the solid lines (15°C) and the dashed lines (30°C) show exemplary the target pressure at different ambient temperatures. The black lines illustrate the refueling end pressure which is reached after the subsequent H_2 admixture. Note that all points on the black lines (solid and dashed) represent end pressures for HCNG-mixtures with the same energy content.

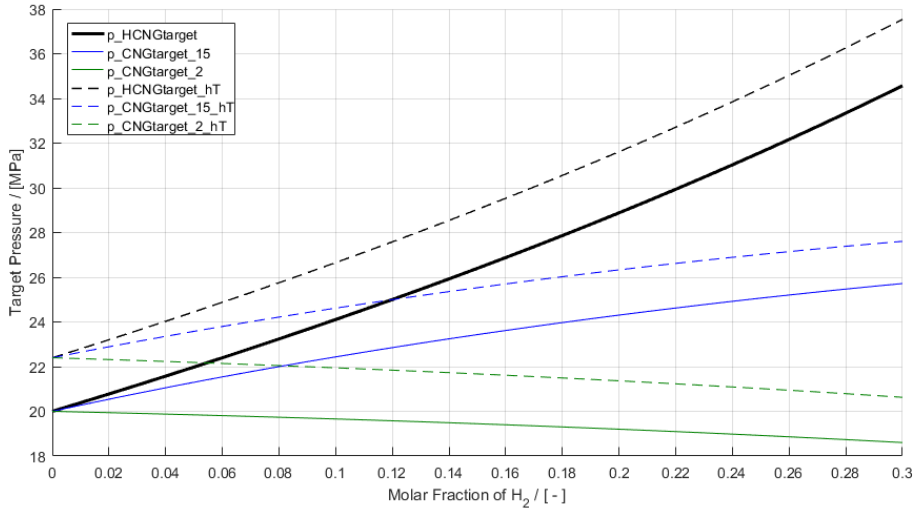

Fig. 31 CNG target pressures (colored) and refueling end pressures (black) in dependence of H_2 fraction, initial car tank pressure and ambient temperature

The calculated target pressures shown above do not account for compression heat release. Separate correction values based on empirical formulas from Atlas Copco and own measurements and simulations are added to include the temperature increase caused by compression. In addition to abovementioned parameters this correction value also depends on refueling time.

As an example the gas temperature inside the car tank can increase in the order of 50°C when refueling a HCNG-mixture with 25 vol-% of H_2 due to compression heat release. This requires the target pressure to be increased very significantly by around 10 MPa. By adding this value to the target pressures shown in the diagram above one can recognize that complete refueling will not be possible at high ambient temperatures and high H_2 fractions at the Empa dispenser. The pressure in the Empa dispenser is limited to 40 MPa due to some of the installed components. This means that in such cases CNG refueling needs to be stopped early by the control unit to ensure that enough H_2 can still be added subsequently. Otherwise the predefined mixture cannot be met.

It is important to note that temperature increase due to compression heat release is not only critical regarding material limits of the car tank but also regarding the available storage pressure or the pressure limits of the components installed in the dispenser. If the energy content within the car tank is to remain equal for all plausible ambient temperatures and H_2 fractions up to 30 vol-%, the dispenser would need to be able to operate up to pressures of 45 – 50 MPa. Whereas a further increase of the H_2 fraction may make sense with respect to emissions and efficiency of an HCNG vehicle the dispensing of such mixtures becomes significantly more complex. To avoid damaging car tanks and high storage tank pressures precooling of the mixture may become necessary when refueling with higher H_2 contents.

HCNG refueling data

The functionality of the HCNG dispenser was tested on a single cylinder first. It was equipped with piping and fittings that allowed the connection to the fueling nozzle and the emptying of the cylinder between tests.

During the subsequent first refueling of the actual test vehicle with HCNG, data from both the vehicle and the dispenser were recorded. For this refueling the H_2 fraction was set to 25 vol-%. The initial tank pressure was 2 MPa and ambient temperature amounted to 23°C. The diagram below shows the measured car tank pressures for each of the five tanks of the test vehicle during refueling. Thereby, the pressure sensor is placed in the tank valve rather than inside the tank which explains why the pressure curves decrease to equal value in between the pressure pulses in the beginning. The green dots represent pressure measurements within the dispenser hose (recorded with only 1 Hz).

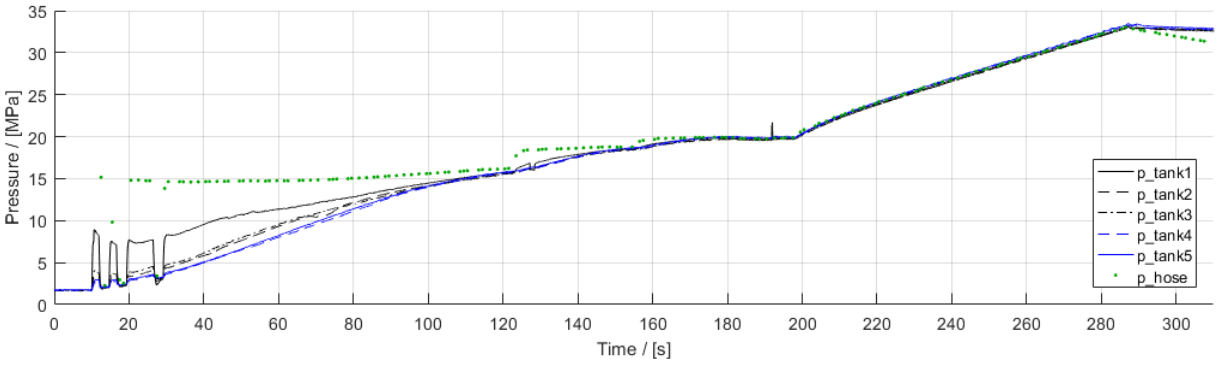

Fig. 32 Measured pressures for each of the five tanks of the test vehicle (black and blue) and the fueling hose (green) during refueling

CNG is refueled from around 10 s to 180 s whereas H_2 refueling starts at about 192 s and ends at 287 s. The complete refueling process took approximately 4.5 minutes. Note the pressure drops between hose and the individual car tanks in the beginning of the refueling. As refueling proceeds and CNG mass flow decreases also the pressure differences between the tanks diminish.

Furthermore the gas temperature within the vehicle tanks was measured as depicted in the subsequent diagram. The temperature drop below ambient temperature caused by the Joule-Thomson effect in the beginning which is typical for CNG refueling is not evident in this case. A possible explanation could be related to the location of the temperature sensor and the gas entrance within the vehicle tank. Presumably the cooling effect due to the quasi isenthalpic expansion is mostly limited to the region of the gas entrance and only reaches the temperature sensor in a weakened form.

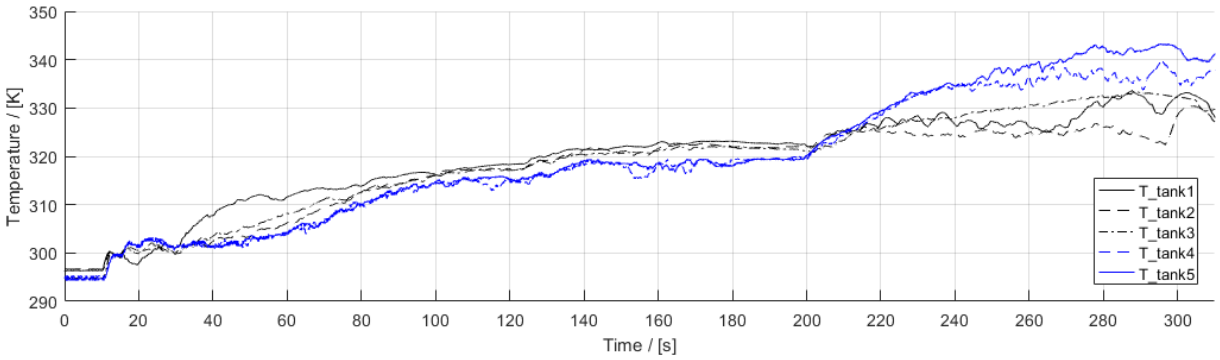

Fig. 33 Measured temperatures for each of the five tanks of the test vehicle

Figure 33 shows an increase in gas temperature of almost 50°C for vehicle tank 5. It is noticeable that temperatures in tank 4 and 5 which are furthest away from the receptacle rise to the highest temperature values while H_2 is refueled. Also the increase in temperature at around 200 s starts a few seconds earlier. This is an indication that the tanks 1-3 received a greater amount of gas during the CNG refueling part and therefore take up less in the H_2 refueling part which results in different individual H_2 fractions for each tank. For instance, tank 5 should therefore contain a higher H_2 fraction than tank 1. According to very basic investigations conducted during this project, this will not pose a problem for the operation of the vehicle. Due to low gas mass flow in the fuel lines while driving each tank will supply a similar amount of its contents to the engine, so that differences in H_2 fractions are equalized in the common fuel line.

With the realization of the HCNG dispenser according to the predefined specifications the objectives are successfully met. As stated above, further works allowing more in-depth investigations regarding the temperature and heat transfer development within the vehicle tanks are already in planning. This topic was identified as crucial to develop control algorithms for the refueling process of gaseous fuels. Furthermore, potential for further work lies in the optimization of the HCNG dispenser regarding the noises emitted while refueling. Particularly during H_2 refueling and when the hose is depressurized unpleasant noises are present which have no relevance regarding safety or functionality but could lead to concerned users.

3.3. HCNG vehicle field testing

Field test with standard CNG vehicles

Three vehicles of the company Mobility Solution AG, now called Post Company Cars AG, were equipped with data loggers which were configured to record various engine parameters during a field test phase. With each vehicle, baseline measurements were carried out on the chassis dynamometer at Empa focusing on emissions and fuel consumption.

Thereafter, the vehicles were in use about 3 months in normal operation with CNG and where used as parcel delivery vehicles. After this phase, the vehicles were successively switched to HCNG operation (2 Vol-% H_2), fuelled at the ad interims HCNG-refuelling station. The vehicles have been measured again on the chassis dynamometer after some run in time. The vehicles completed their field testing phase at the end of August 2015.

Fig. 34 Fiat Ducato from the Mobility Solution AG on the chassis dyno at Empa

These vehicles are mainly used in the parcel distribution service and therefore have a high number of motor starts per day. The data from the field test shows an average of over 30 starts a day, with a maximum of 87 engine starts on one day. 7'600 engine starts with CNG and 10'500 engine starts with HCNG (2 Vol-% H2) have been evaluated. On average, 95% of the engine starts are carried out at an engine coolant temperature higher than 80°C.

The evaluation also included an analysis of engine start times. One of the results of this analysis was the time delay from the first turn of the engine starter (crank) and the first firing of the first cylinder (CTFF) derived from engine speed measurements during start-up. Four different delays were distinguished:

- Very short; CTFF smaller than 100ms
- Short, CTFF between 100ms and 200ms
- Normal, CTFF between 200ms and 400ms
- Long, CTFF bigger than 400ms

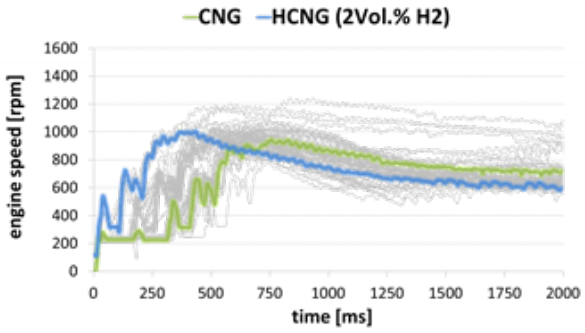

Fig. 34 Various engine start speed traces with examples for CNG and HCNG

HCNG compared to CNG operation shows a shift to shorter crank to first fire times (see figure below). This can be explained with the higher ignition quality caused by the hydrogen in the HCNG blend. Even small amounts of hydrogen seem to have an impact on start quality.

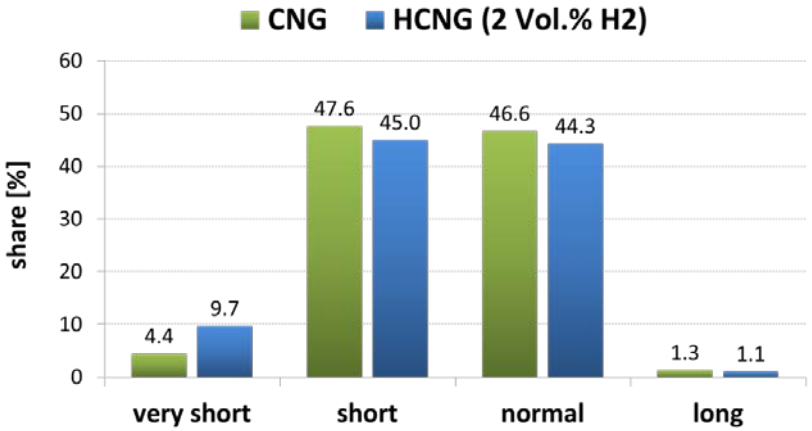

Fig. 35 Start time distribution for CNG and HCNG (average of three vehicles and a total of 18'100 engine starts)

Chassis dyno measurements with standard CNG vehicles

With each vehicle base measurements were carried out on the chassis dynamometer with CNG and also with HCNG (2 Vol-% H_2) as fuel. As driving cycle for these measurements, the CADC cycle from the Artemis program has been used. This cycle corresponds to a real world driving cycles with three phases (urban, rural, highway).

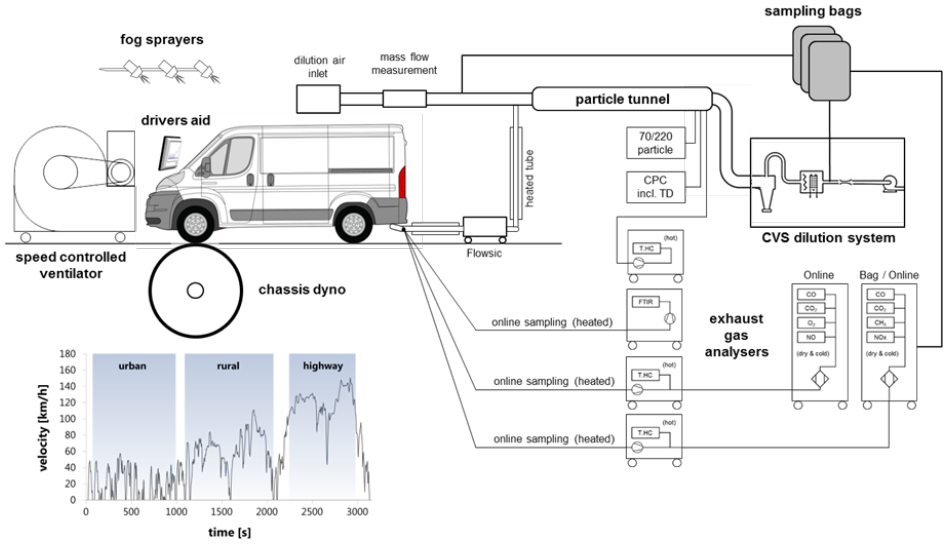

Fig. 36 Measurement setup and Artemis CADC speed profile

The emission values for carbon monoxide (CO), nitrogen oxides (NOx) and unburned hydrocarbons (T.HC) show no significant differences between the two types of fuel. However, the 2 Vol.-% H_2 blending shows a slight reduction of CO_2 emissions of 1 - 1.5%, which can be explained by the reduced carbon content of the fuel as well as a slight improvement of the engine efficiency.

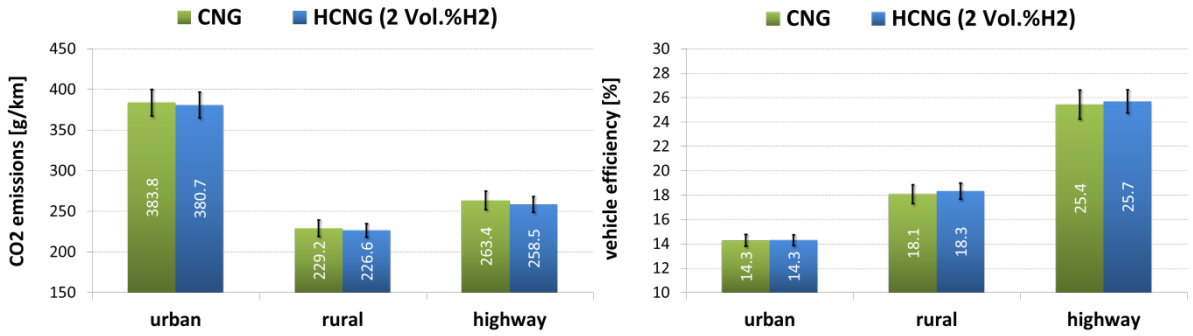

Fig. 37 Average CO_2 emissions (CADC sub cycles, error bars represent the standard deviation) and vehicle efficiency (tank to wheel, error bars represent the standard deviation)

The slight efficiency increase can be explained by the improved ignition phase. Such effects have already been observed at Empa in other HCNG projects. In the current case, however, they are very faint due to the low blending of hydrogen. In the overall evaluation, it can be stated that all three vehicles did not show any negative characteristics during the field test as well as during the chassis dyno tests. Therefore raising the hydrogen content of the natural gas in the grid to the maximum of the allowed value for motor fuel application (2 vol-%) represents a favorable option for the storage of excess electricity and making it available for mass mobility.

Field test with converted HCNG vehicles

Besides the field test with low blending ratios also higher amounts of hydrogen in methane were tested. For this purpose a special demonstration vehicle was built up during the project. The complete fuel system needed to be designed to withstand the hydrogen-induced embrittlement, caused by the diffusion of atomic hydrogen in the steel.

It was intended to finish the rebuild until the beginning of 2016, but as mentioned earlier, the sub project experienced severe delays in the supply chain of the hydrogen compatible fuel system parts.

At first it was planned to equip the vehicle with 200 bar type 4 CNG bottles to reduce the vehicles empty weight and offer the desired resistance to hydrogen. But refueling simulations showed that the driving range is reduced when hydrogen is added to natural gas due to the lower volumetric energy density of the mixture. To maintain or even extend the driving range also with higher hydrogen blending ratios a concept to set the maximum pressure for HCNG refueling to 350bar was worked out. Hydrogen resistant 350bar bottles are used in different industrial applications, but were not available in the specific dimensions for this vehicle application. Therefore it was decided to switch to 700bar bottles normally used for fuel cell vehicles. The 700 bar type 4 hydrogen cylinders where delivered in April 2016.

In parallel to the procurement of the hydrogen cylinders, enquiries for the rest of the fuel line parts were made. Since the cylinder valves must fit on the cylinders, it was necessary to procure 700bar hydrogen valves. New pressure regulators were needed to reduce the tank pressure from 350bar to the fuel rail pressure of 7bar, and they also needed to be hydrogen and CNG proof.

Clarifications, the quotation and ordering process was time consuming since all the parts where ordered from US and Canadian Manufacturers. These kinds of parts are no stock items and were specially fabricated on order. The last parts where delivered in the beginning of February 2017 and the rebuild was completed by the end of July 2017.

The final fuel system consists of 5 70MPa 36L hydrogen cylinders, each with hydrogen cylinder valve with pressure and temperature sensors. The new stainless steel fuel lines bring the gaseous fuel to the first pressure regulator at the back of the vehicle where the cylinder pressure is lowered to a medium pressure of 70bar. In the front of the vehicle sits another pressure regulator which reduces the medium pressure to the low pressure of 7bar in the fuel rail. To compensate the temperature drop due to the pressure reduction over the regulators and in order to prevent their seals from being damaged due to low temperature, several countermeasures were implemented. Both pressure regulators and a part of the fuel line are electrically heated and a helical 35 meter fuel line was added as a heat exchanger in the rear of the vehicle. The last part is the new stainless steel fuel rail holds the original fuel injectors which are actuated by the unaltered ECU. In this configuration the fuel system has been certified by the SVGW and the vehicle was approved for on-road operation by the STVA of Zürich.

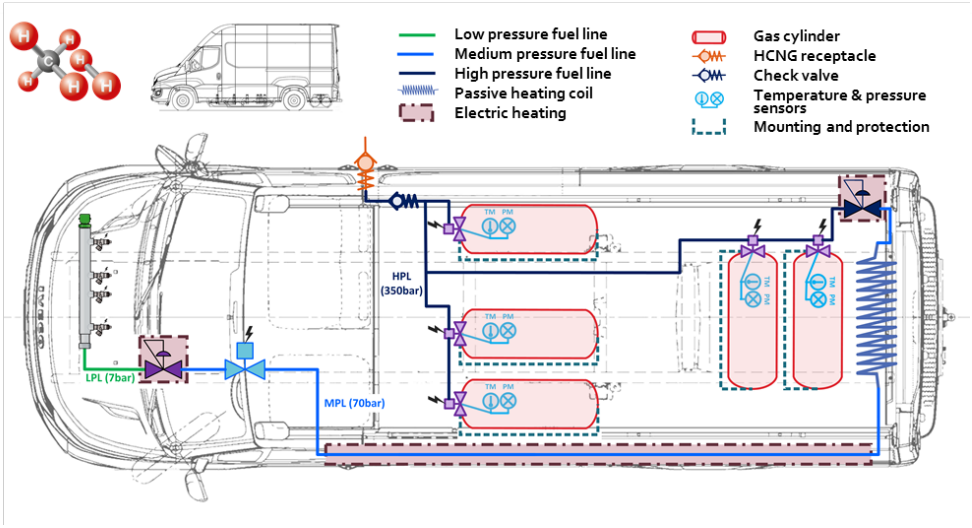

Fig. 38 Overview of the system components of the HCNG fuel system

The vehicle started its field test in August 2017 and is running until the current day without problems and the interaction between petrol station and vehicle works properly. Since the fuel lines are designed with a wider diameter then the original system, the re-fueling times of the new fuel system are similar to the durations of the conventional, non-modified vehicle. The field test will continue until spring 2018 and will be completed with additional chassis dyno tests to analyze the fuel consumption and emission behavior of the vehicle concept.

This demonstrator vehicle shows that with minor changes in the fuel system, of which some are already part of the latest state of technology for CNG vehicles, current natural gas vehicles are capable of running with renewable fuel produced with fluctuating excess electricity with lower CO_2 emissions and higher energy efficiency.

3.4. HCNG decentralized power (co-)generation

An engine test bench for emulating conditions relevant for a hydrogen enriched natural gas powered micro combined heat and power (mCHP) plant is shown in Fig. 39. The single cylinder 4-stroke naturally aspirated SI engine is equipped with a lambda controller for lean burn operation as well as with a gas mixing device to apply hydrogen addition to the methane fuel and synthetic EGR (only applied for stoichiometric operating points) using CO_2 and N_2 (see Fig. 40). The engine torque is measured using an eddy current brake. In addition the engine is fully indicated which allows for heat release calculations of multiple consecutive single cycles. The coefficient of variation of peak pressure or indicated mean effective pressure (IMEP) is used to judge combustion stability. Other characteristic parameters such as crank angles after spark timing at certain heat release are relevant and are extracted also from the data recorded on this test bench.

The influence of hydrogen addition on the emissions is quantified using an exhaust gas analysis system which measures volume concentrations of NO_x, HC, CO, O_2 and CO_2.

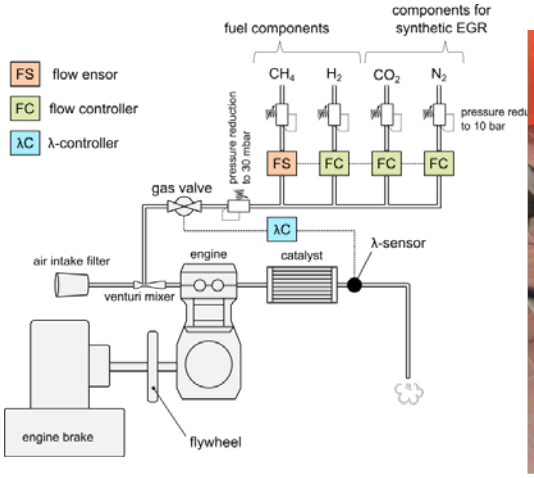

Fig. 39 Test bench schematic

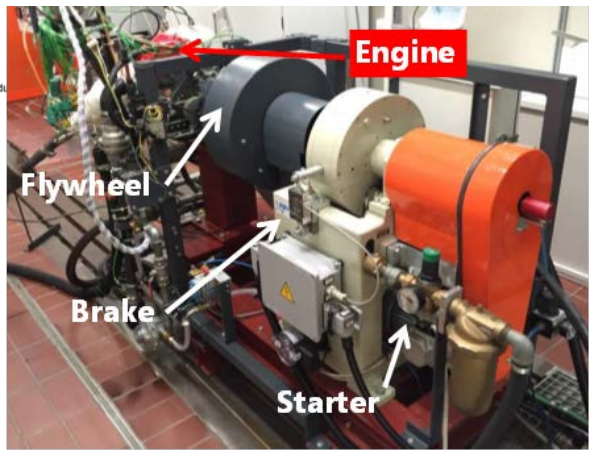

Fig. 40 Test bench with eddy current brake, flywheel and the 250ccm naturally aspirated mCHP engine.

<u>H_2 introduction</u>

Micro CHP plants are operated from the gas grid where the fuel pressure is as low as 20-40 mbar. Therefore as a relevant introduction method of H_2 the premixing of NG, H_2 and air in a venturi mixer is implemented in this case. In a similar manner the low pressure synthetic EGR is introduced, see Fig. 39. Like this a homogeneous pre-mixed condition is reached at spark timing.

Spark plug concepts

The smallest pre-chamber spark plugs available on the market are of size M14. The spark plug thread size in the investigated engine is M10 and due to close by cooling channels it is not possible to cut an M14 thread into the same Cylinder head. The remaining wall thickness at the weakest point would only be roughly 0.75mm (see Figure 41). The tolerances of the cast cylinder head are not exactly known and therefore the risk of damaging the cooling channel with an M14 thread is too big. Open-chamber spark plugs are investigated using hydrogen addition to promote stable combustion and short inflammation phases.

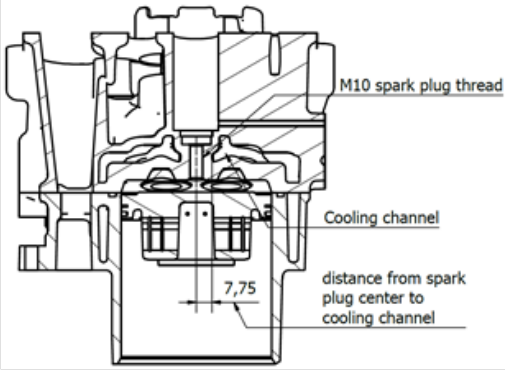

Fig. 41 Sectional drawing of the cylinder head.

Operation limits

For both the lean burn - and the EGR engine operation the according limits are investigated by steadily increasing the lambda or the EGR content respectively for a certain CH_4/H_2 mixture until misfiring happens or the torque collapses. The fuel mixtures investigated are 0, 10, 25 and 50% volume share of hydrogen in methane (see first column in Table 10). The coefficient of variation of the indicated mean effective pressure (COV_{IMEP}) serves as a criterion for stable engine operation. An operating point with a COV_{IMEP} < 5% is considered stable.

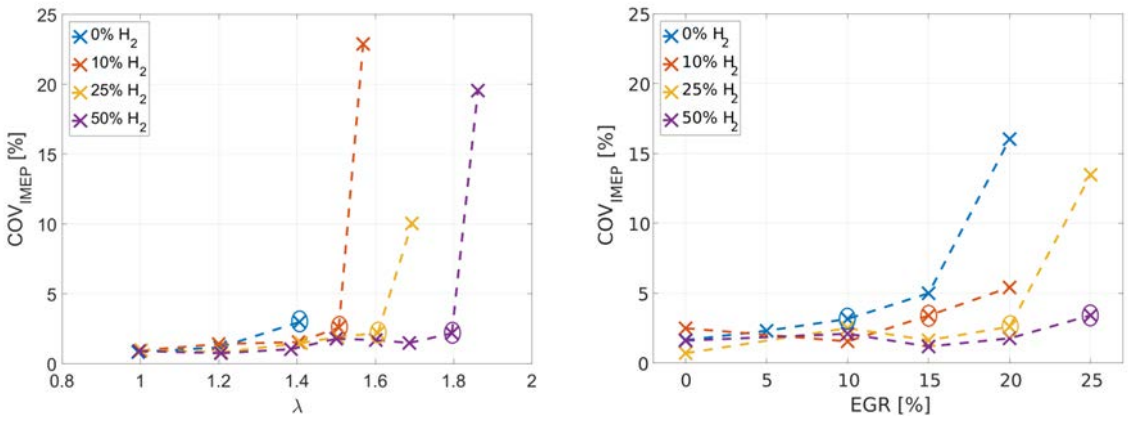

Fig. 42 COVIMEP for lean burn (a) – and EGR (b) operation. The points marked with a circle represent the operating limit for the according fuel mixture

Figures 42 show the COV_{IMEP} for all operating points in the lean burn - and EGR operation campaign respectively. For the lambda variation as well as for the EGR variation a drastic increase of COV_{IMEP} is observed beyond a limiting value λ_{lim} or EGR_{lim} respectively, where COV_{IMEP} is still below 5%. This behavior is observed for each fuel mixture investigated. By increasing the hydrogen content of the fuel however, the operating limits are pushed towards higher lambdas or EGR contents respectively. Table 5.3 shows the operating limits of each fuel mixture.

Tab. 10 Operating limits (COVIMEP < 5%) for lean burn – and EGR operation displayed for each of the fuel mixtures used. The eight operating points shown here correspond to the ones marked with a circle in Fig. 5.18.

Fuel mixture [H_2 $\%_{vol.}$]	λ_{lim} [-]	EGR_{lim} [%]
0	1.4	10
10	1.5	15
25	1.6	20
50	1.8	≥25[1]

[1] The fuel mixture with 50% hydrogen could not be tested with higher EGR rates due to flow limitations in the gas valve.

Efficiency:

Figure 43 (a) and (b) illustrate the engine efficiency of the set-up shown in Figure 42 for lean burn – and EGR operating conditions respectively. For all fuel mixtures and lean burn operation the efficiency decreases progressively with increasing lambda until the operation limit (marked with a circle) is reached. A steep drop in efficiency can be observed beyond the operation limit. For $\lambda \geq 1.2$ an increasingly positive influence of hydrogen addition is observable for increasing lambdas.

In contrast to the lean burn operation, a clear benefit of hydrogen addition for the EGR operation is not apparent for EGR rates below the operating limit. Compared to the lean burn operation a rather mellow decrease in engine efficiency for increasing EGR rates below the operating limit is observed (see Figure 43 (b)). Therefore in general the limits of EGR operation indicate a higher efficiency than the corresponding limits of the lean burn operation.

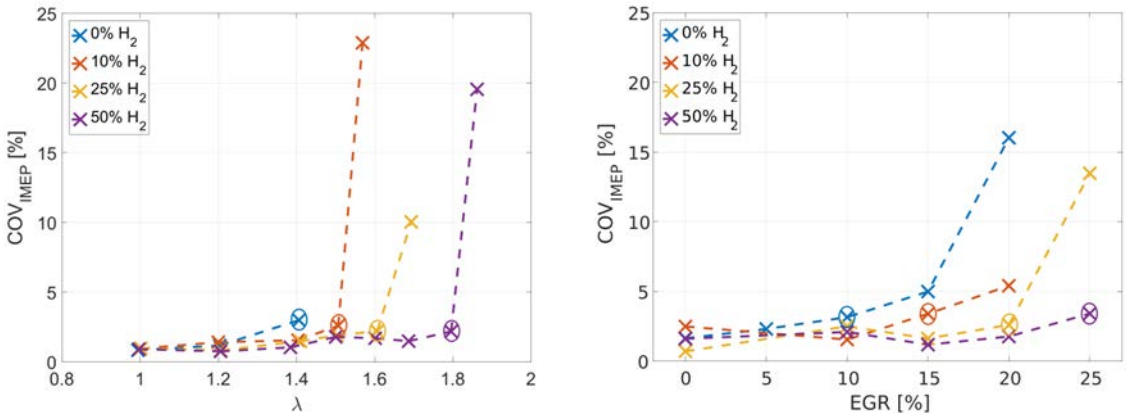

Fig. 43 Engine efficiency for lean burn (a) – and EGR (b) operation. The operating limits for each fuel mixture (see table 1) is marked with a circle.

Raw emissions:

Lean burn – as well as EGR operation is applied for raw NO_x emission reduction in cases where only an oxicat is installed for exhaust gas after treatment. For both concepts the NO_x emissions are more reduced the leaner the engine is operated or the more EGR is applied. In the next section only the operating limits shown in Table 10 are discussed in further detail because they represent the operating point with the minimum emissions for each fuel mixture.

Figure 44 shows the raw emissions for the lean burn operating limits. By adding up to 50% hydrogen to the fuel mixture it is possible to increase the operating lambda to 1.8 and therefore reduce the raw NO_x emissions by 92% down to 42 mg/Nm^3 at 5% oxygen dilution compared to 770 mg/Nm^3 for the best case with CH_4–only-operation. The NO_x emission limit for stationary gas IC engines of a fuel power ≤ 100kW is 250[2] mg/Nm^3.

With 232 mg/Nm^3 the raw NO_x emissions of the operating point with $\lambda = 1.6$ and a hydrogen content in the fuel of 25% fall below this limit. The legal limit for carbon monoxide emissions are 650[2] mg/Nm^3 while HC emissions are not regulated. For a mCHP application the carbon monoxide emissions must in any case be reduced using appropriate exhaust gas after treatment. They moderately increase with increasing lambda due to incomplete combustion. The HC emissions almost stay constant due to the cancelling out of both the positive and the negative effect on the quenching distance of the hydrogen addition and the increasing lambda respectively.

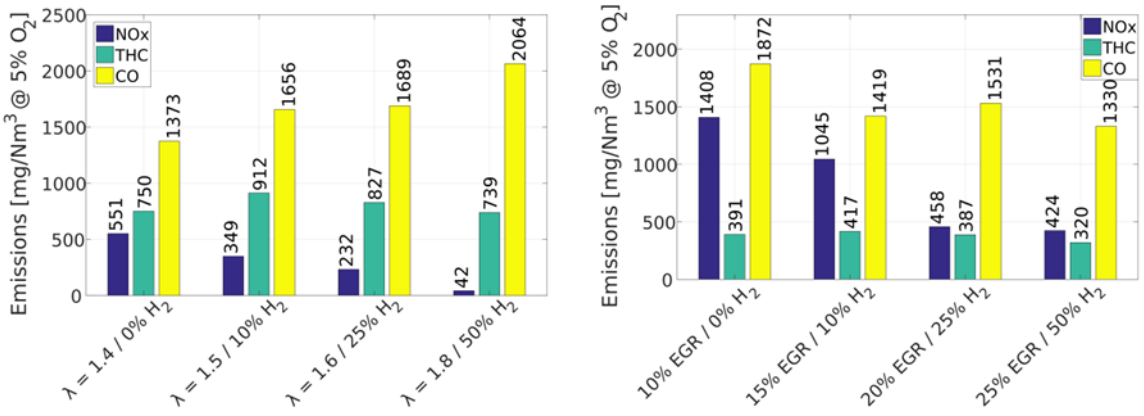

Fig. 44 Raw emissions for the operating limits of the lean burn (a) – and EGR (b) operation

The raw emissions for the EGR operating limits are illustrated in Figure 5.20 (b). Here the hydrogen addition allows for extending the EGR rate from 10 to at least 25%[1] while the NO_x emissions only reduce by 70% down to 424 mg/Nm^3 which is not enough to satisfy the LRV[2].

[2] Luftreihalte-Verordnung (LRV) vom 16. Dezember 1985 (Stand am 1. April 2017)

H_2 addition applied to a stoichiometric mCHP plant with TWC – field testing:

The same fuel mixtures as in the above described engine experiments are applied to the mCHP plant Aladin II. This is a system where a three way catalyst (TWC) and stoichiometric operation are implemented to minimize the NO_x, CO and HC emissions. Regardless on the hydrogen share in the fuel, all emissions are below 30 mg/Nm^3 at 5% oxygen dilution. Also in terms of electrical (32%) and thermal (57%) efficiency no dependencies on the hydrogen share can be observed.

3.5. Publications / patens

Paper in preparation

3.6. Industrial and institutional WP3 partners

▪ SFOE (BFE)	Swiss federal office of energy
FOGA	Research, development and promotion fund of the Swiss gas industry
▪ Atlas Copco	Industrial (gas) company Support regarding the development of the HCNG dispenser. Extended collaboration within the project “Future Mobility Demonstrator” which is linked to RENERG^2 WP4
▪ Endress+Hauser	Instrumentation and process automation company Collaboration in the field of mass flow metering (Coriolis). A substantial part of gaseous fuel dispensing.
▪ Mobility Solutions AG	Corporate fleet manager (fleet of Post AG) Providing and operating of test vehicles for field testing
▪ Iveco / FPT AG	Powertrain technologies company Collaboration regarding the adaption of CNG-vehicles for HCNG use
▪ SwissAuto	Engine company Support on CHP test engine
▪ Motorex	Lubricant company Information exchange with respect to permissible engine lubricants for hydrogen enriched fuels

4. Acknowledgements

The project team would like to express special thanks of gratitude to the Swiss Federal Office for Energy (SFOE) for the support and funding of the project.